Two études$^{\text{(time permitting)}}$ on unexpected behaviour of drift-wave turbulence (in MAST) near the stability threshold

Ferdinand van Wyk (Oxford *DPhil 2017*), E. Highcock (Chalmers),
Michael J. Fox (Oxford *DPhil 2017*), A. Field (Culham), Y.-c. Ghim (KAIST),
Greg Colyer (Oxford *DPhil 2017*), C. Roach (Culham),
F. Parra, M. Barnes (Oxford), W. Dorland (Maryland),
Alexander Schekochihin (Oxford)

F. van Wyk et al. 2016, JPP 82, 905820609
F. Van Wyk et al. 2017, PPCF 59, 114003
M. F. J. Fox et al. 2017, PPCF 59, 034002
G. J. Colyer et al. 2017, PPCF 59, 055002

Does Flow Shear Matter?

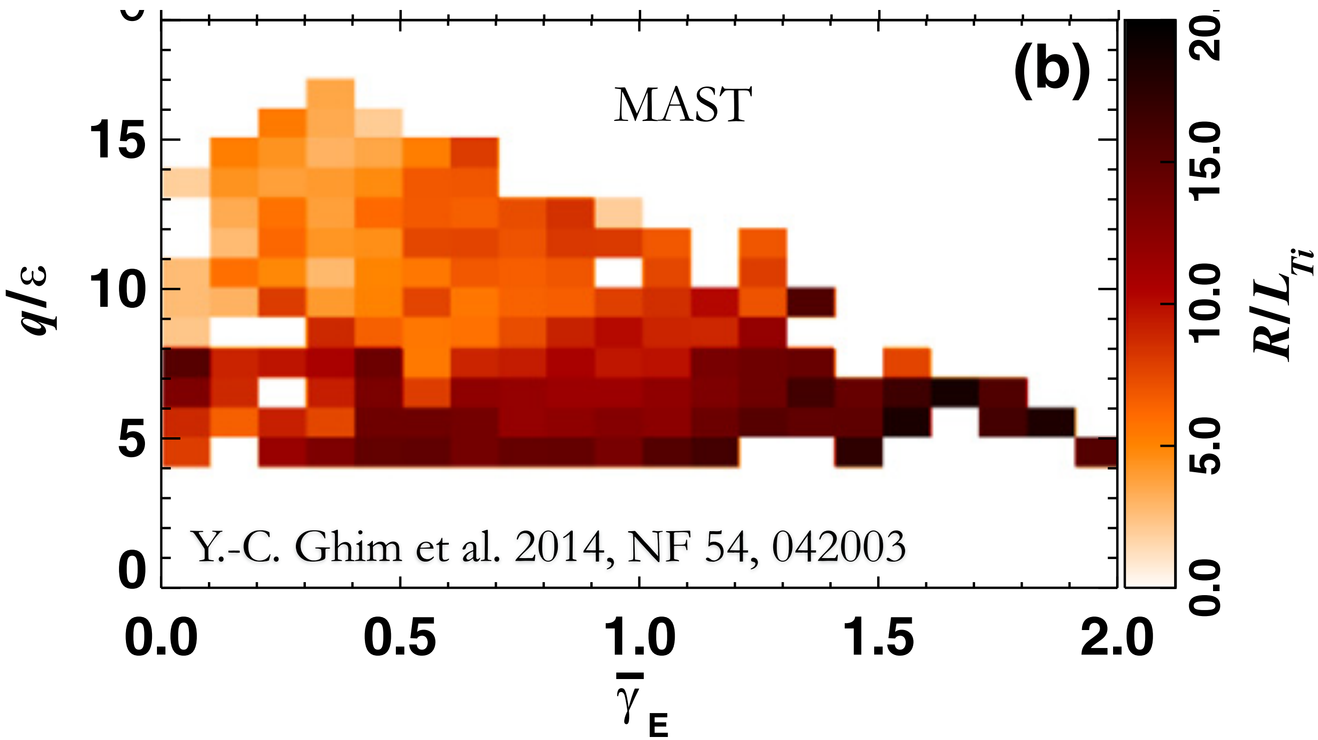

Correlation or causation?

Note: There are good **theoretical reasons** to believe that flow shear changes the threshold [e.g., Newton et al. 2010, PPCF 52, 25001; AAS et al. 2012, PPCF 54, 055011].

There is also **numerical evidence** from CBC simulations [Highcock et al. 2012, PRL 109, 265001].

But do we know this happens in real tokamaks?

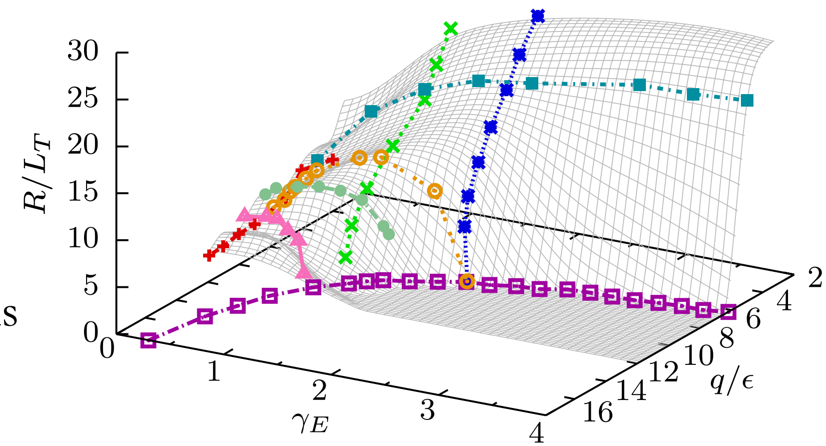

Does Turbulence Know?

Real BES snapshots from MAST:

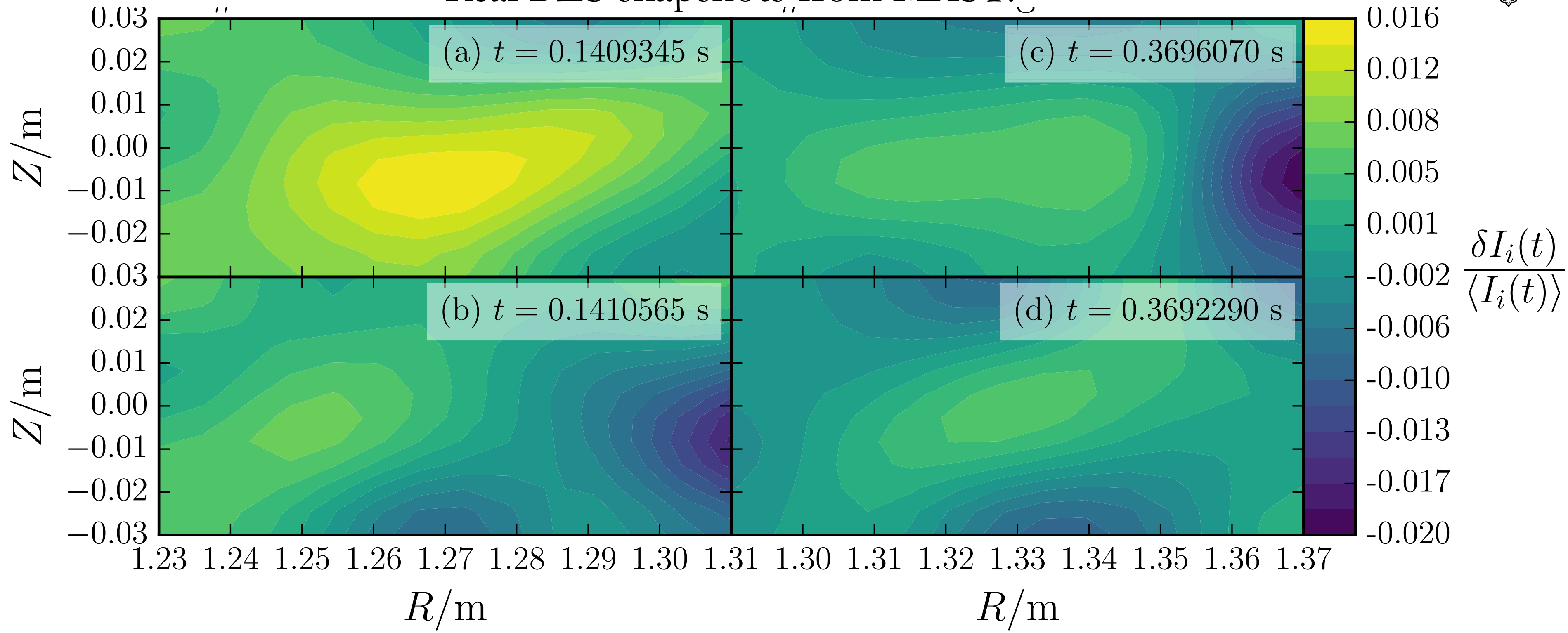

Which of these has flow shear?

Does Turbulence Know?

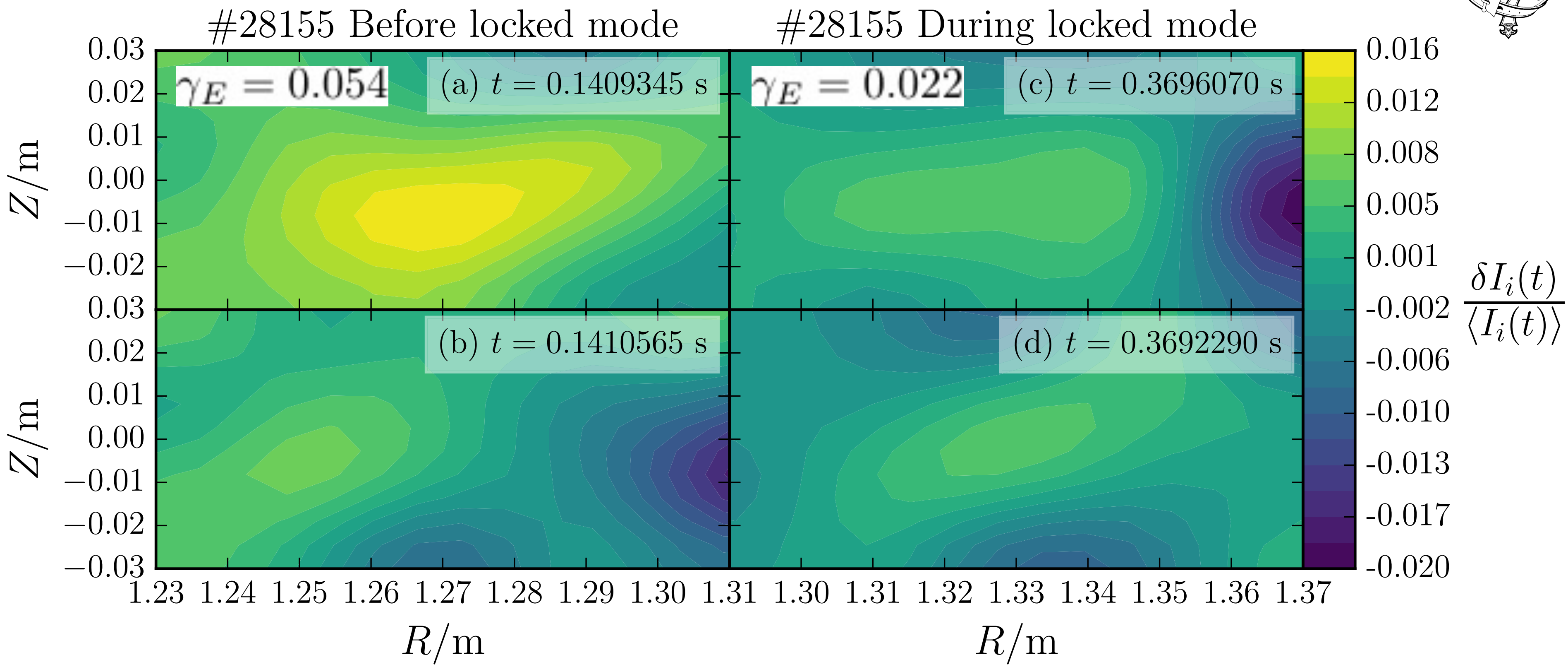

M. F. J. Fox et al. 2017, PPCF 59, 034002

Turbulence Knows, But Does it Care?

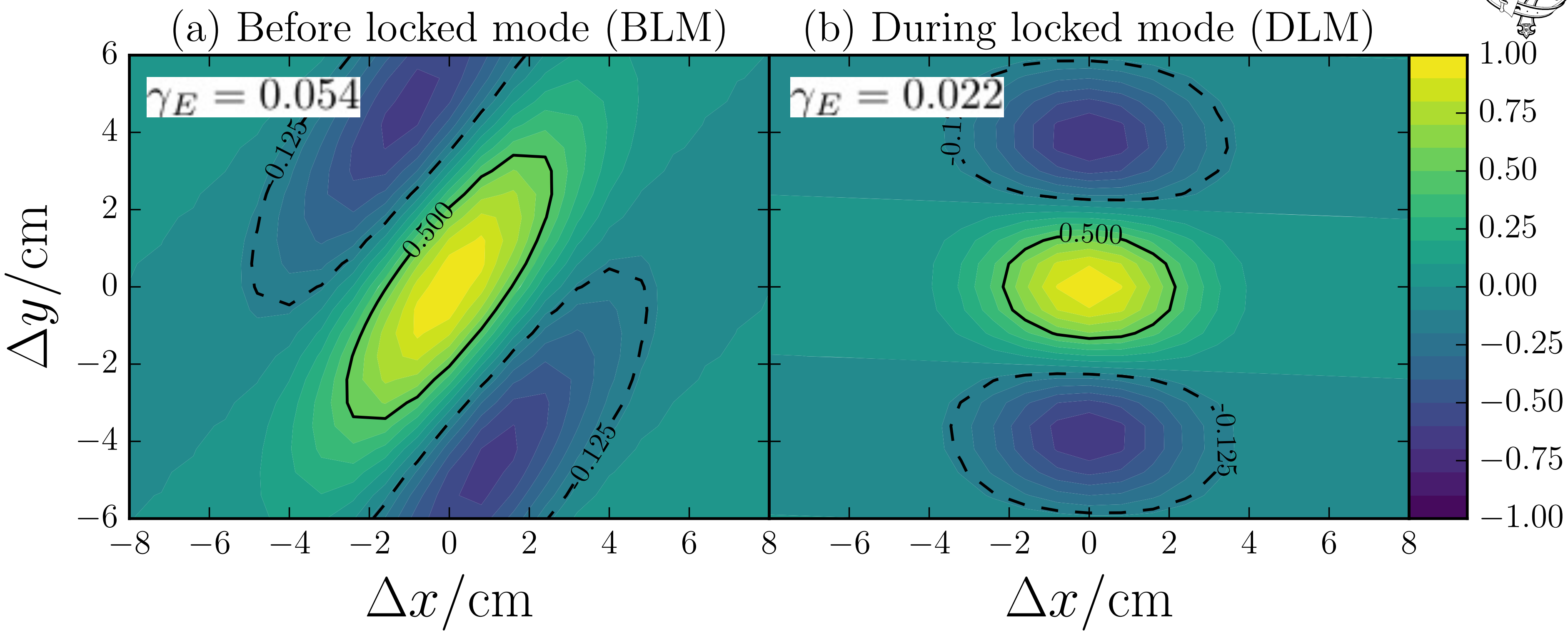

$$C(\Delta x, \Delta y) \sim \exp\left[-\left(\frac{\Delta x}{l_x^2} + \frac{\Delta y}{l_y^2}\right)\right] \cos\left(k_x \Delta x + k_y \Delta y\right)$$

$$k_x(t) = k_x(0) - k_y \gamma_E t \quad \Rightarrow \quad k_x \sim k_y \gamma_E \tau_c$$

$$\boxed{\text{Tilt angle: } \tan\Theta = -\frac{k_x}{k_y} \sim \gamma_E \tau_c}$$

Extracting these from BES data is a lot of work.
Michael Fox developed quite a sophisticated system for this: it is described in exhaustive detail in Fox et al. 2017, PPCF 59, 044008

M. F. J. Fox et al. 2017, PPCF 59, 034002

MAST GK Simulations: Shear is a Stability Parameter

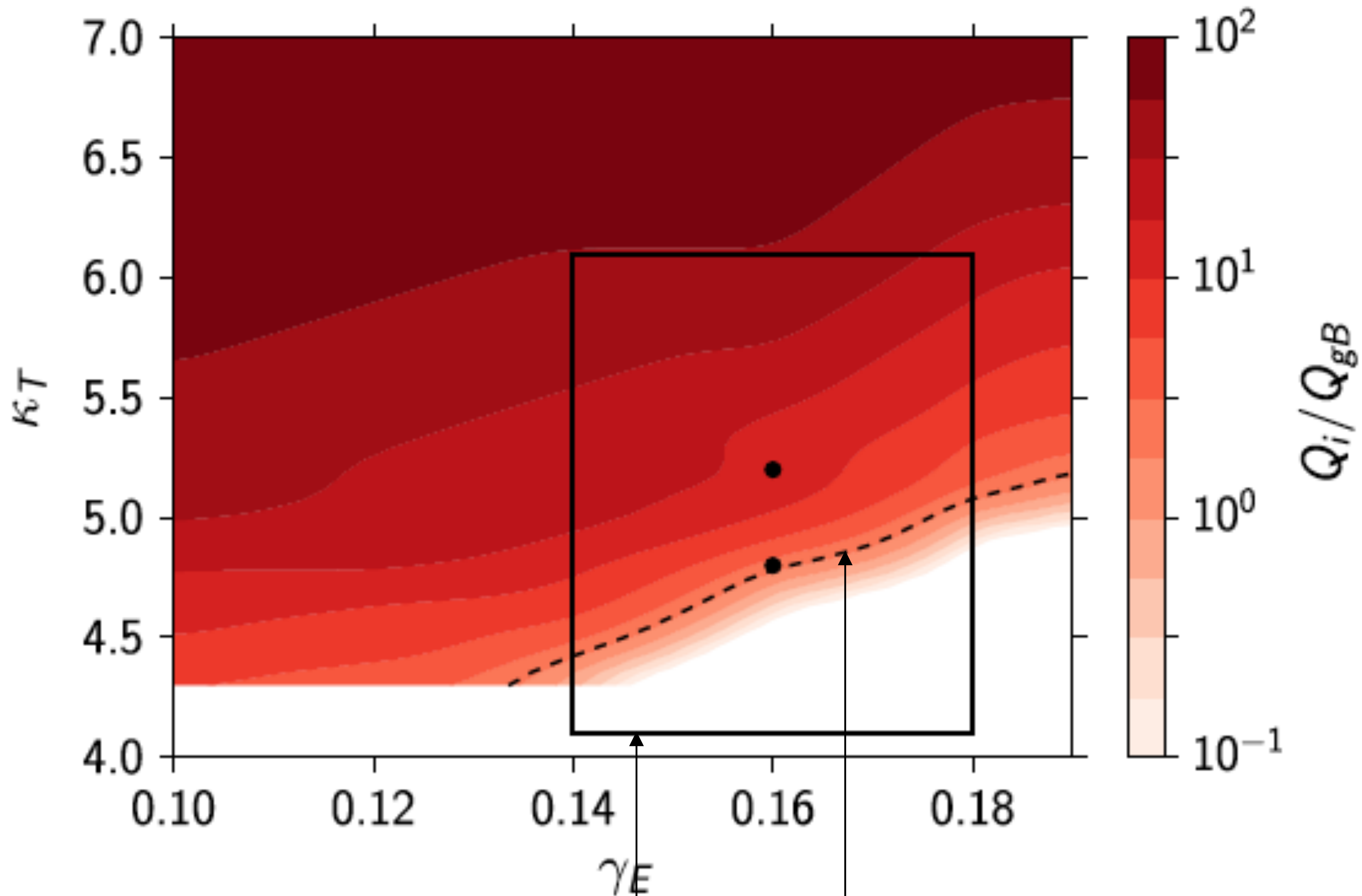

Experiment is close to threshold,
flux changes very rapidly with
equilibrium gradients,
one must simulate a wide range

Experimental value of heat flux
$Q_i/Q_{\mathrm{gB}} = 2 \pm 1$

Experimental-uncertainty range for gradients
$\kappa_T = 5.1 \pm 1, \gamma = 0.16 \pm 0.02$

F. van Wyk et al. 2016, JPP 82, 905820609

MAST GK Simulations: Shear is a Stability Parameter

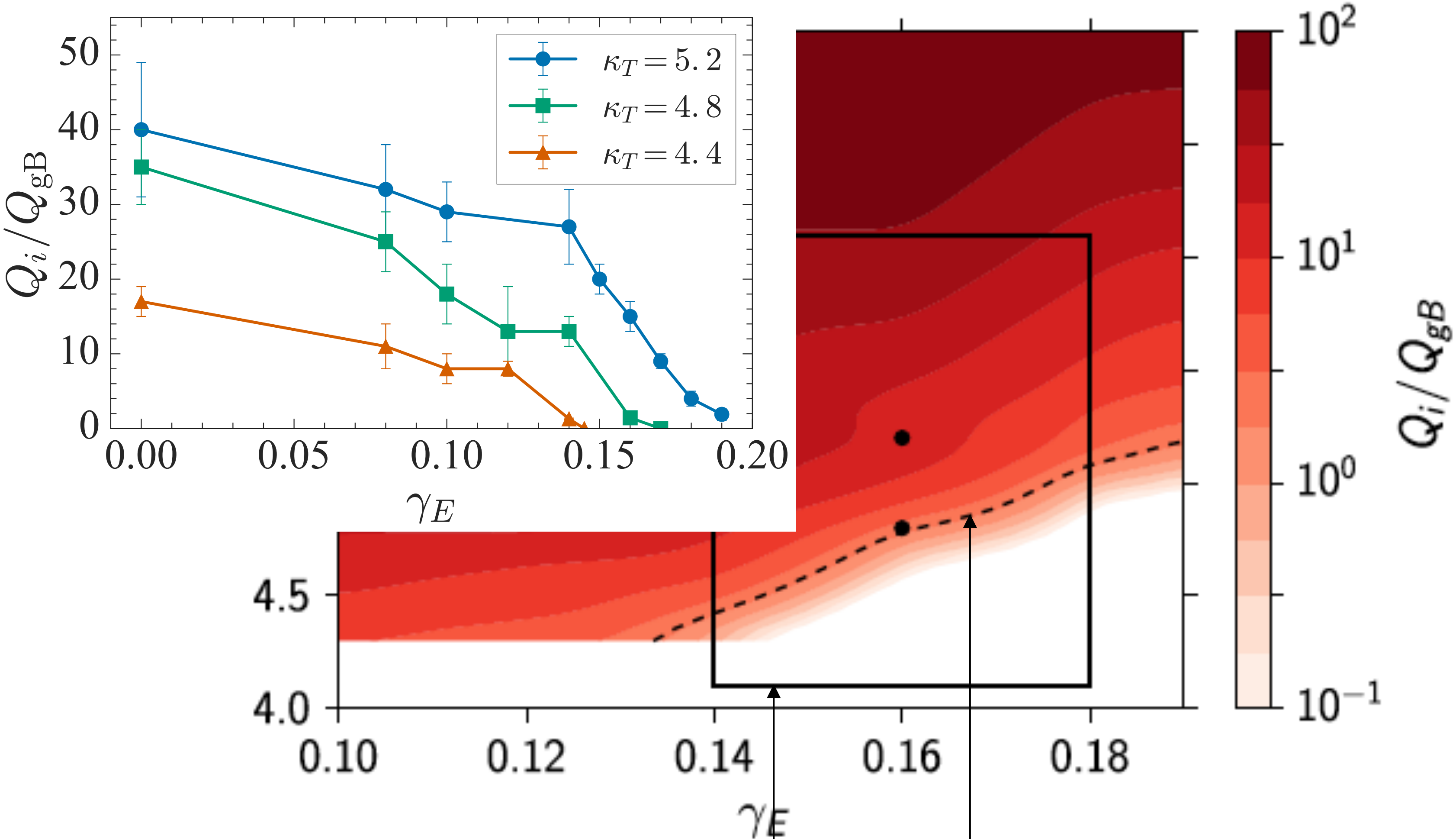

Experiment is close to threshold,
flux changes very rapidly with
equilibrium gradients,
one must simulate a wide range

Experimental value of heat flux
$Q_i/Q_{gB} = 2 \pm 1$

Experimental-uncertainty range for gradients
$\kappa_T = 5.1 \pm 1, \gamma = 0.16 \pm 0.02$

F. Van Wyk et al. 2017, PPCF 59, 114003

MAST GK Simulations: Shear is a Stability Parameter

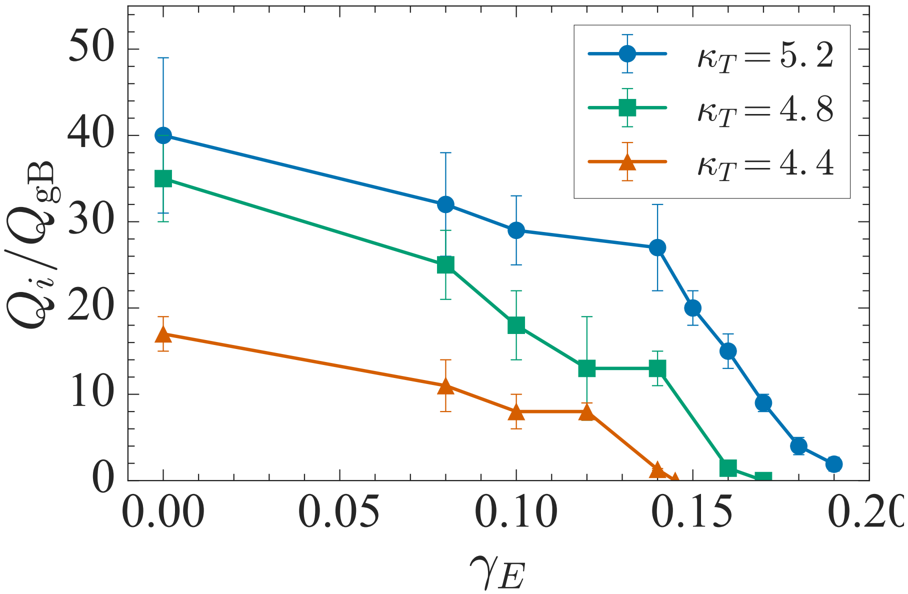

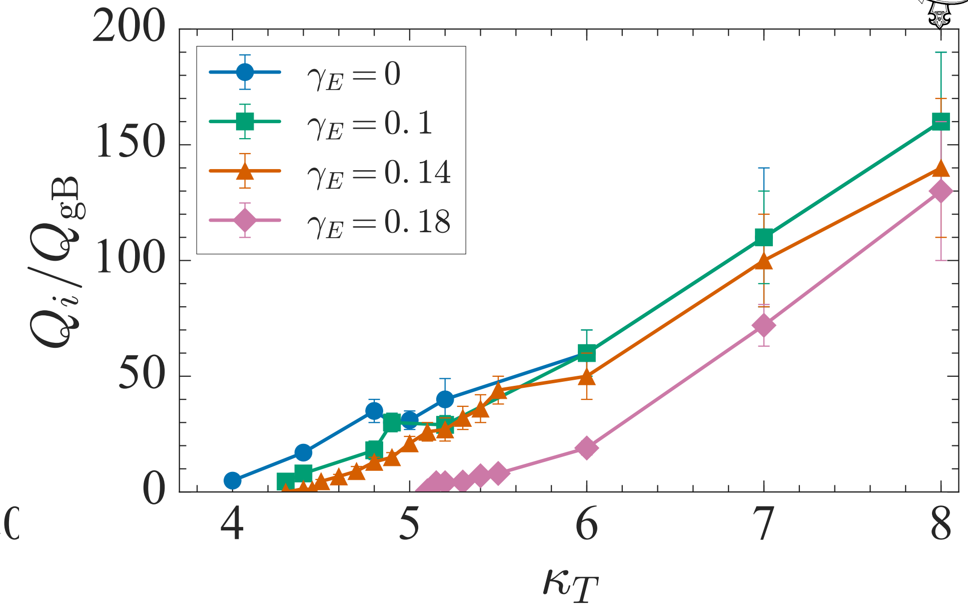

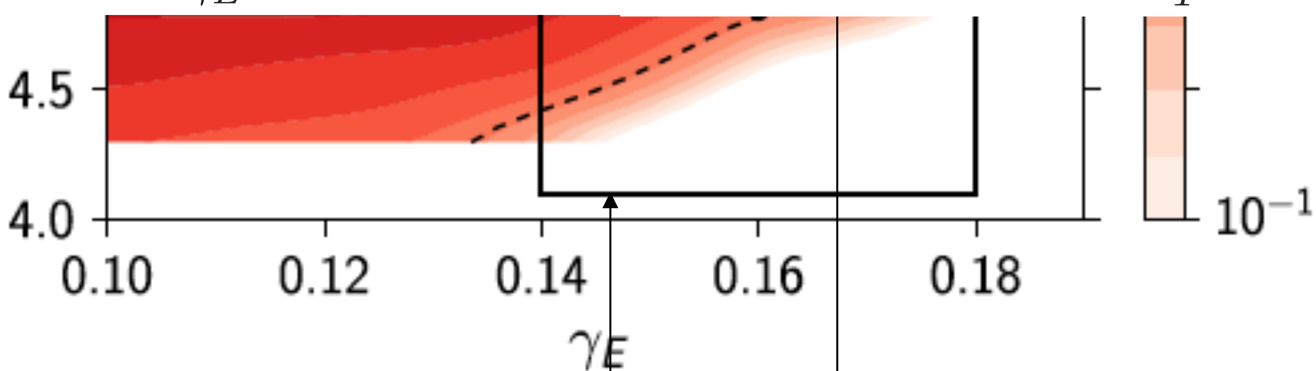

Experiment is close to threshold,
flux changes very rapidly with
equilibrium gradients,
one must simulate a wide range

Experimental value of heat flux
$Q_i/Q_{\rm gB} = 2 \pm 1$

Experimental-uncertainty range for gradients
$\kappa_T = 5.1 \pm 1, \gamma = 0.16 \pm 0.02$

F. Van Wyk et al. 2017, PPCF 59, 114003

Subcritical Turbulence: Threshold is Nonlinear

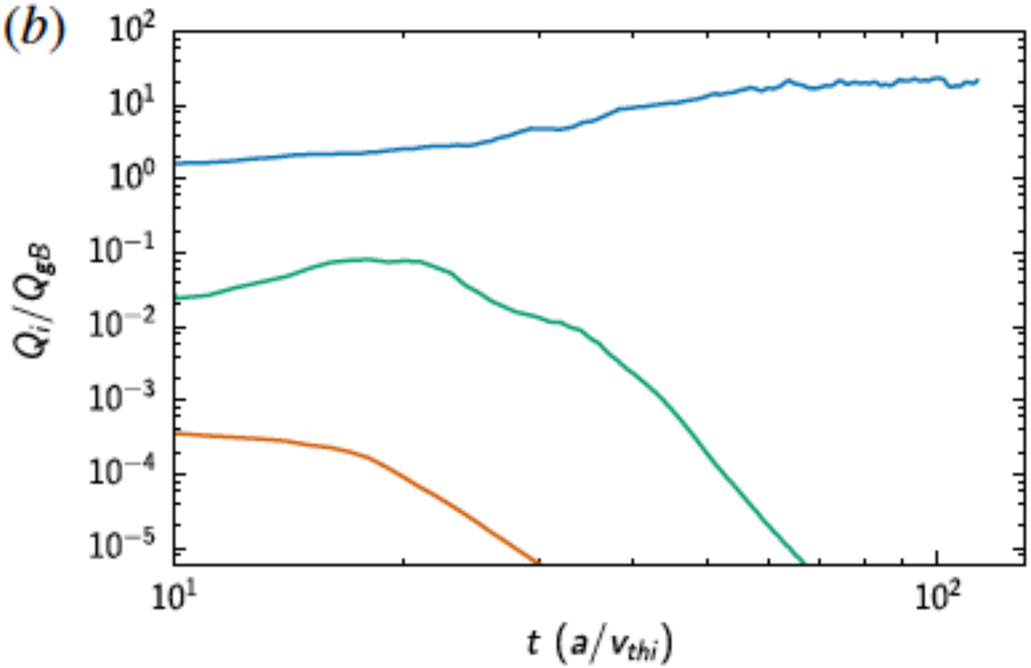

All cases with flow shear are formally linearly stable. Finite initial perturbation needed for a non-zero nonlinear state to be achieved. **Turbulence is subcritical.**

F. van Wyk et al. 2016, JPP 82, 905820609

Subcritical Turbulence: Threshold is Nonlinear

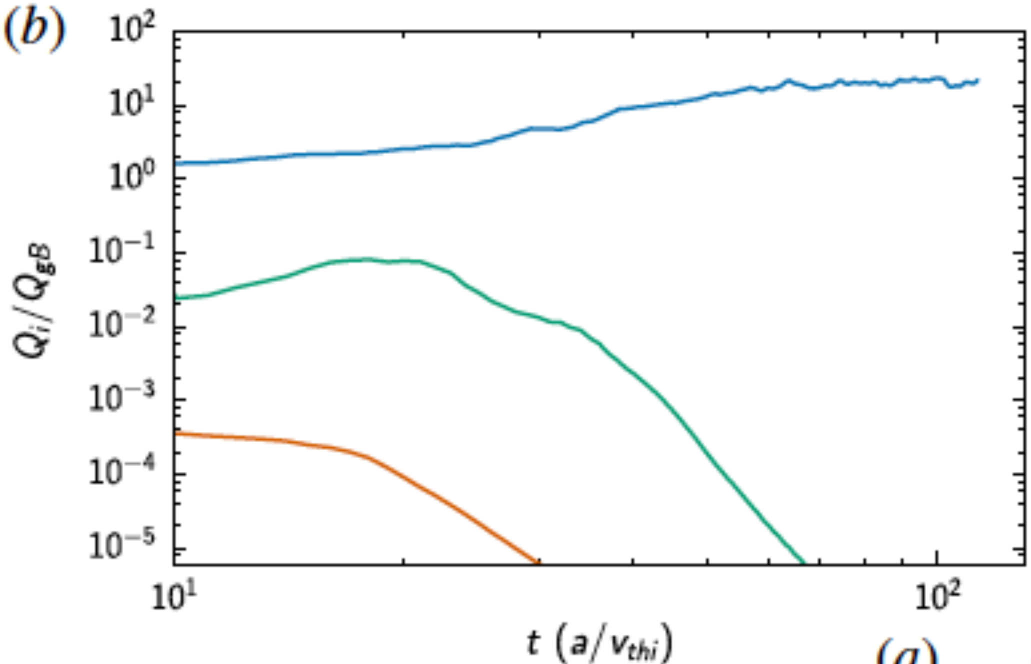

All cases with flow shear are formally linearly stable. Finite initial perturbation needed for a non-zero nonlinear state to be achieved. **Turbulence is subcritical.**

In the linear approximation, perturbations grow transiently. They eventually decay because flow shear pushes k_x to large values:

$$k_x(t) = k_x(0) - k_y \gamma_E t$$

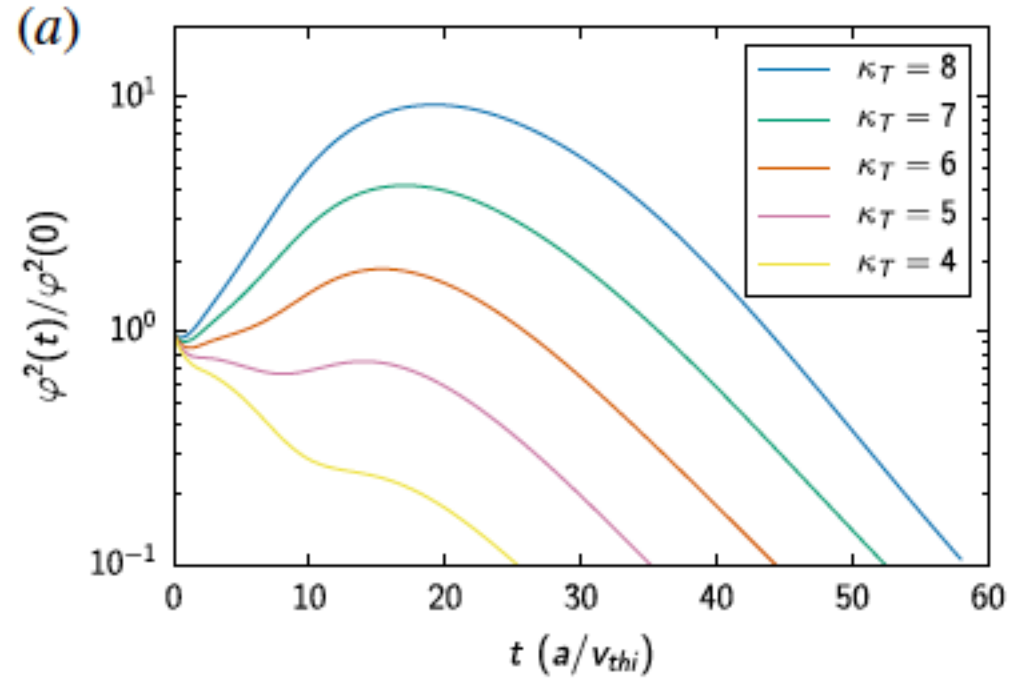

F. van Wyk et al. 2016, JPP 82, 905820609

Away From Threshold: Vanilla ITG

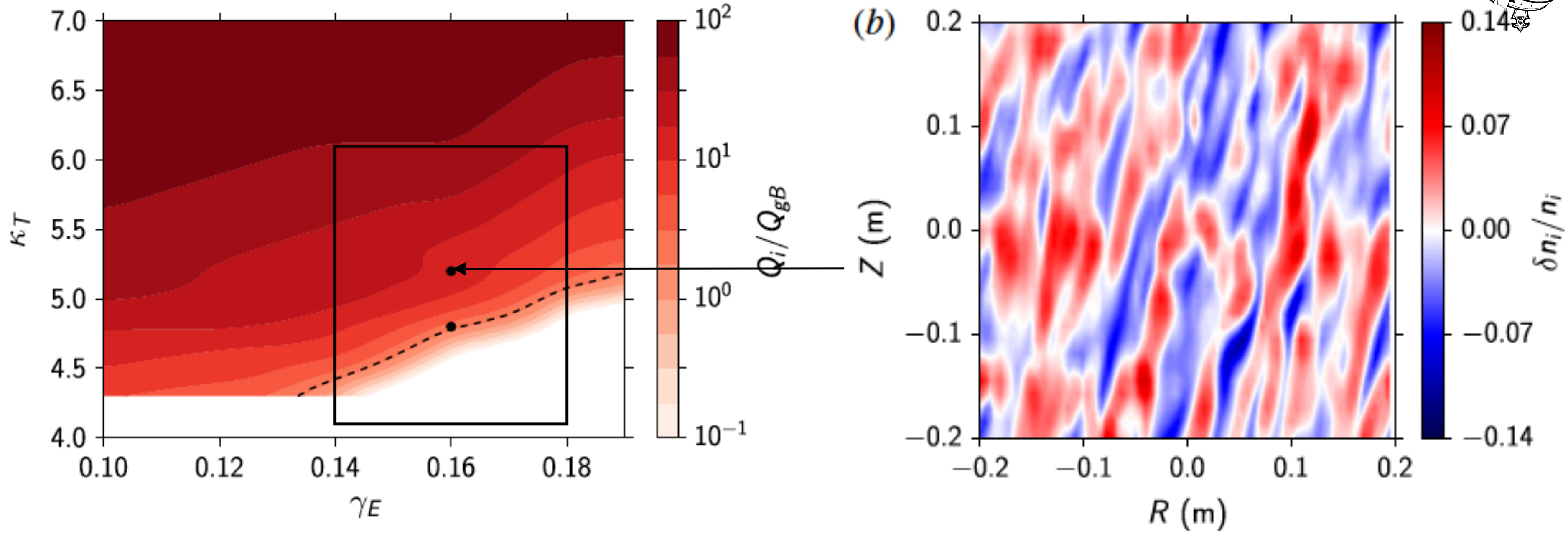

F. van Wyk et al. 2016, JPP 82, 905820609

Near Threshold: Exotic Beasts Roam

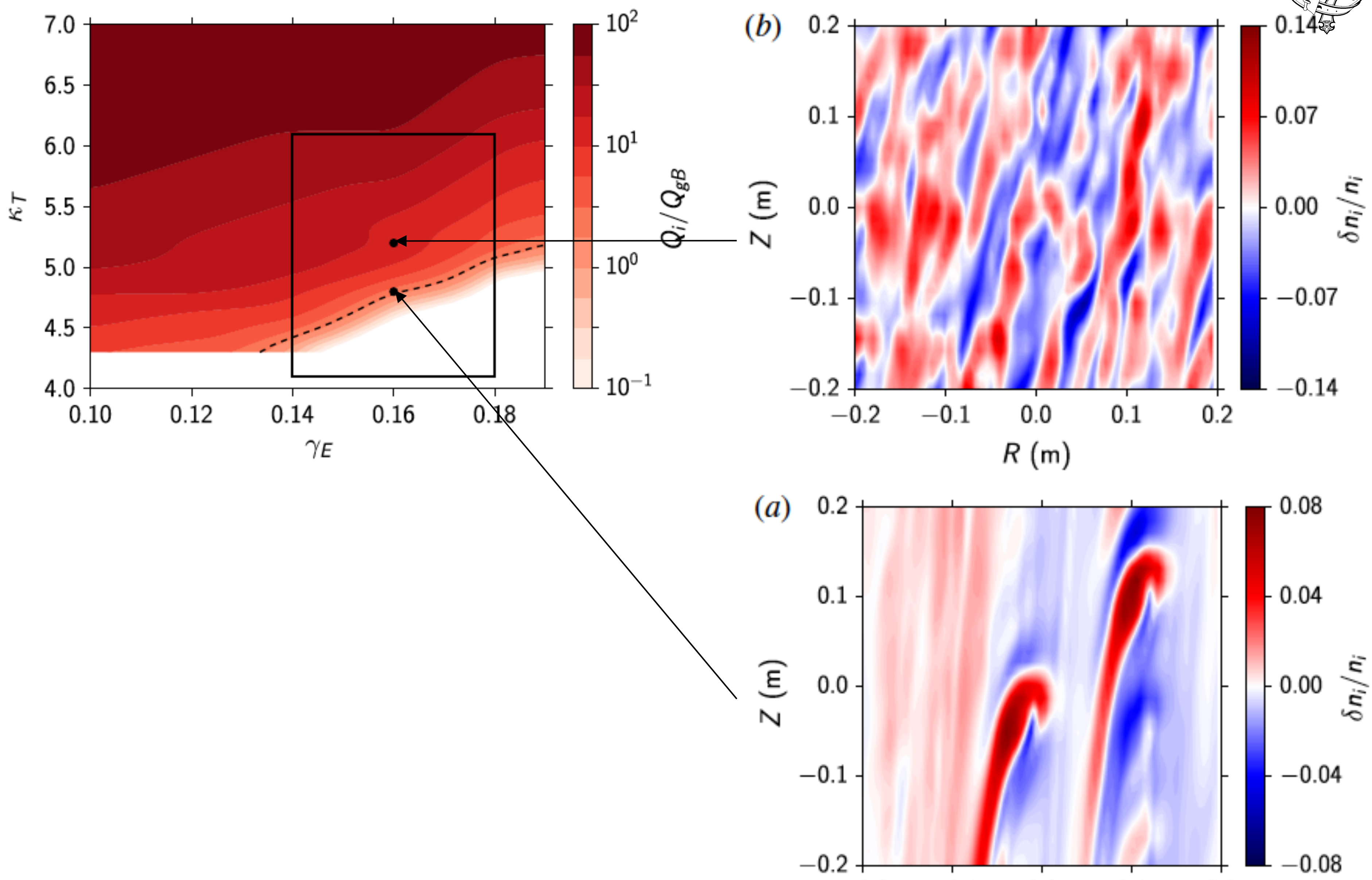

F. van Wyk et al. 2016, JPP 82, 905820609

Structures Live Forever

This is from a simulation
that had only one structure:

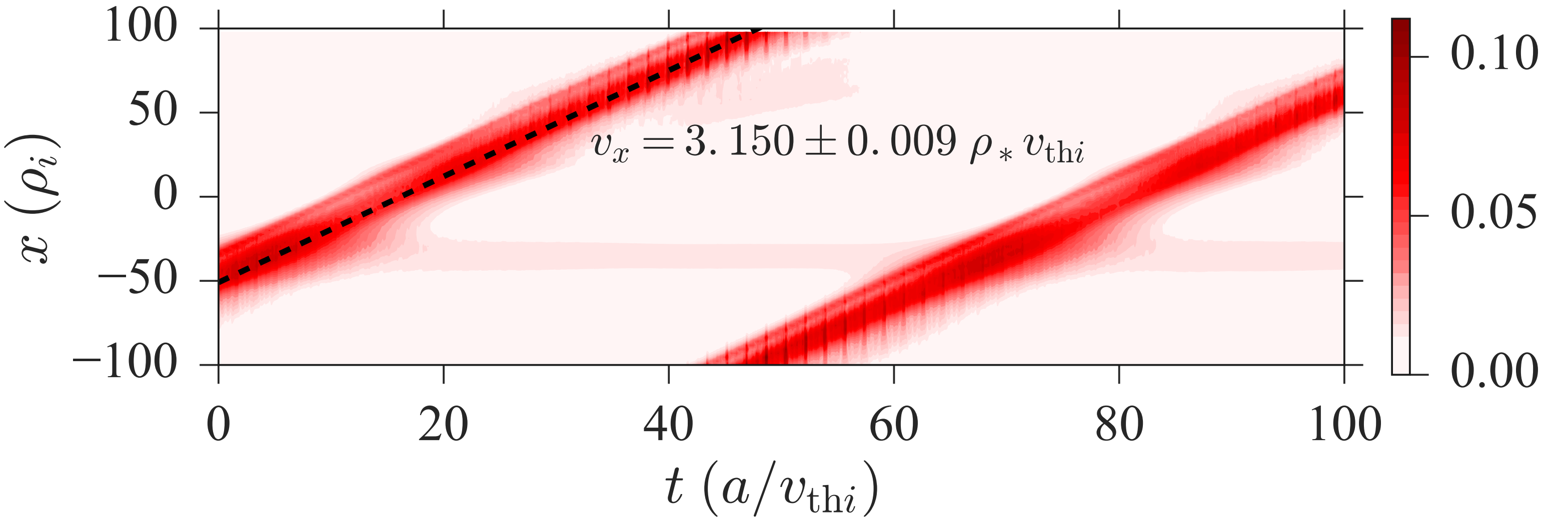

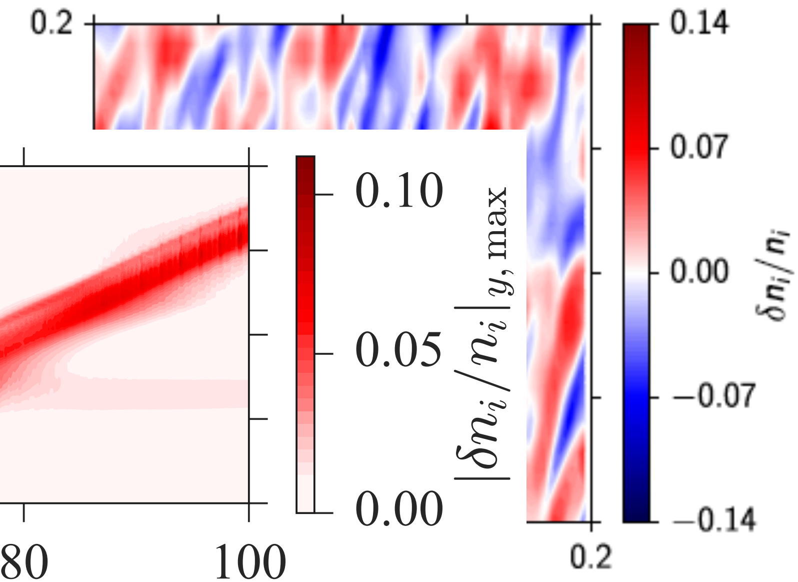

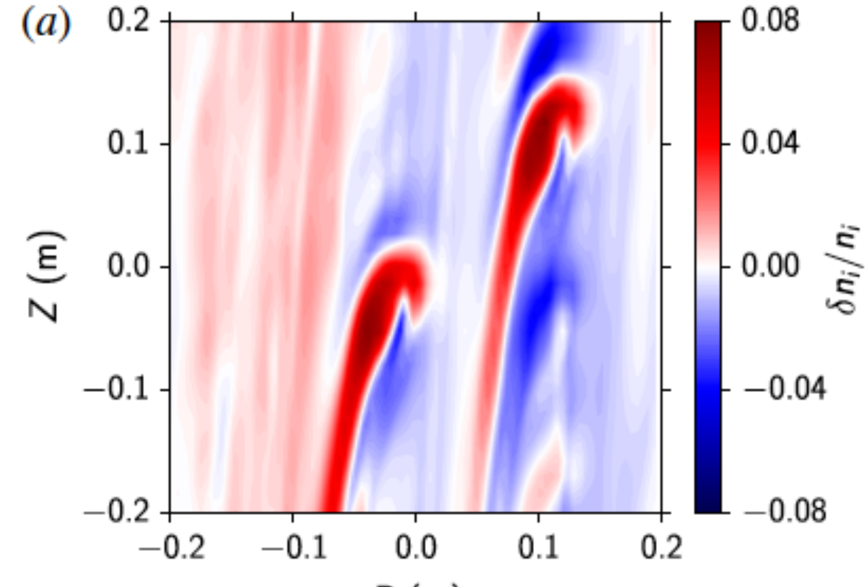

F. Van Wyk et al. 2017, PPCF 59, 114003

Transition by Structure Multiplication

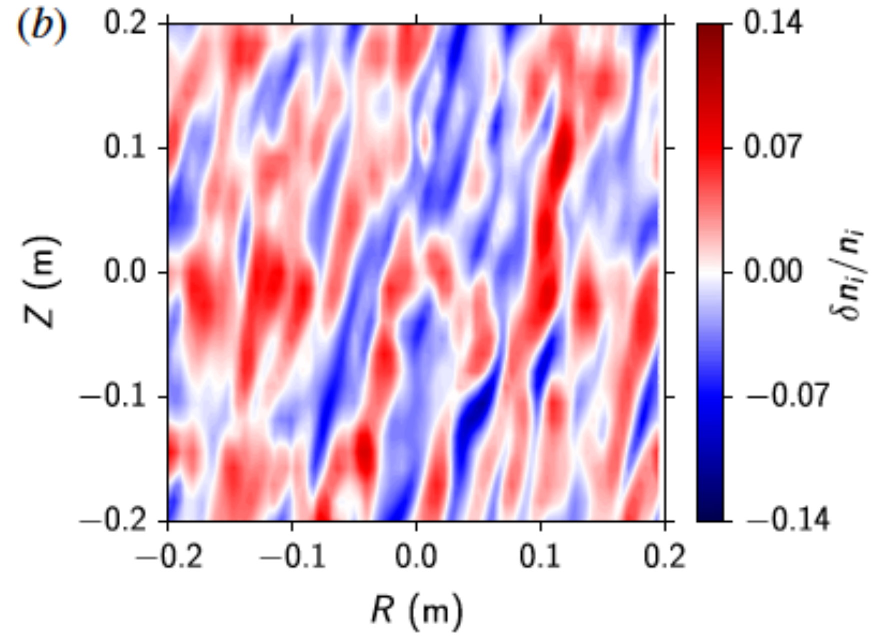

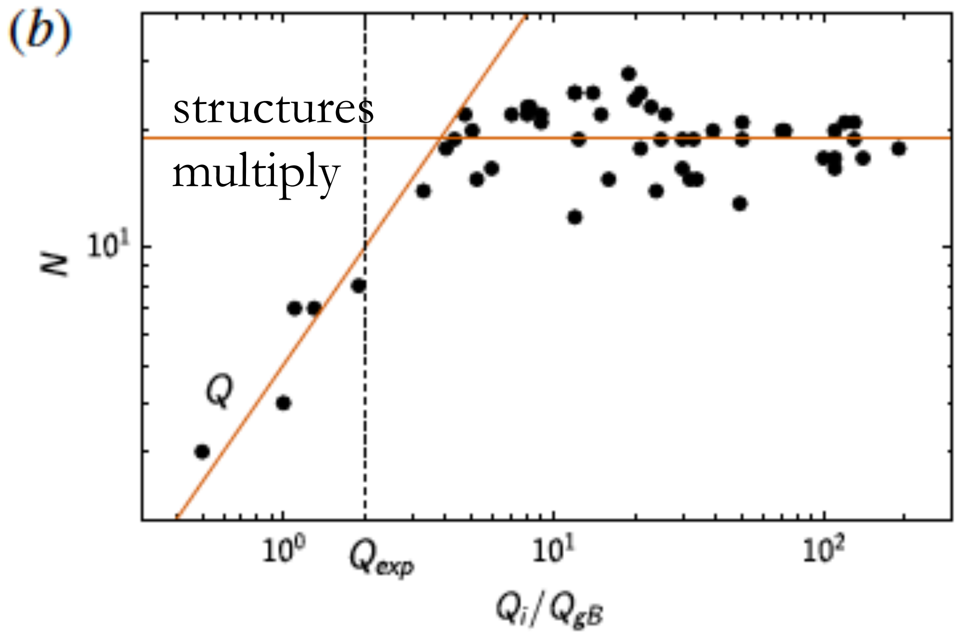

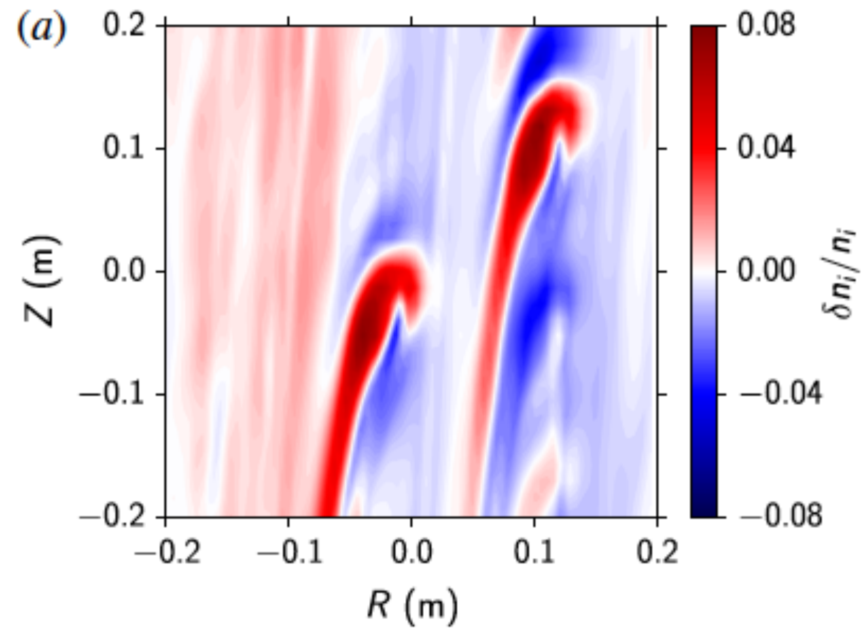

F. van Wyk et al. 2016, JPP 82, 905820609

Transition by Structure Multiplication

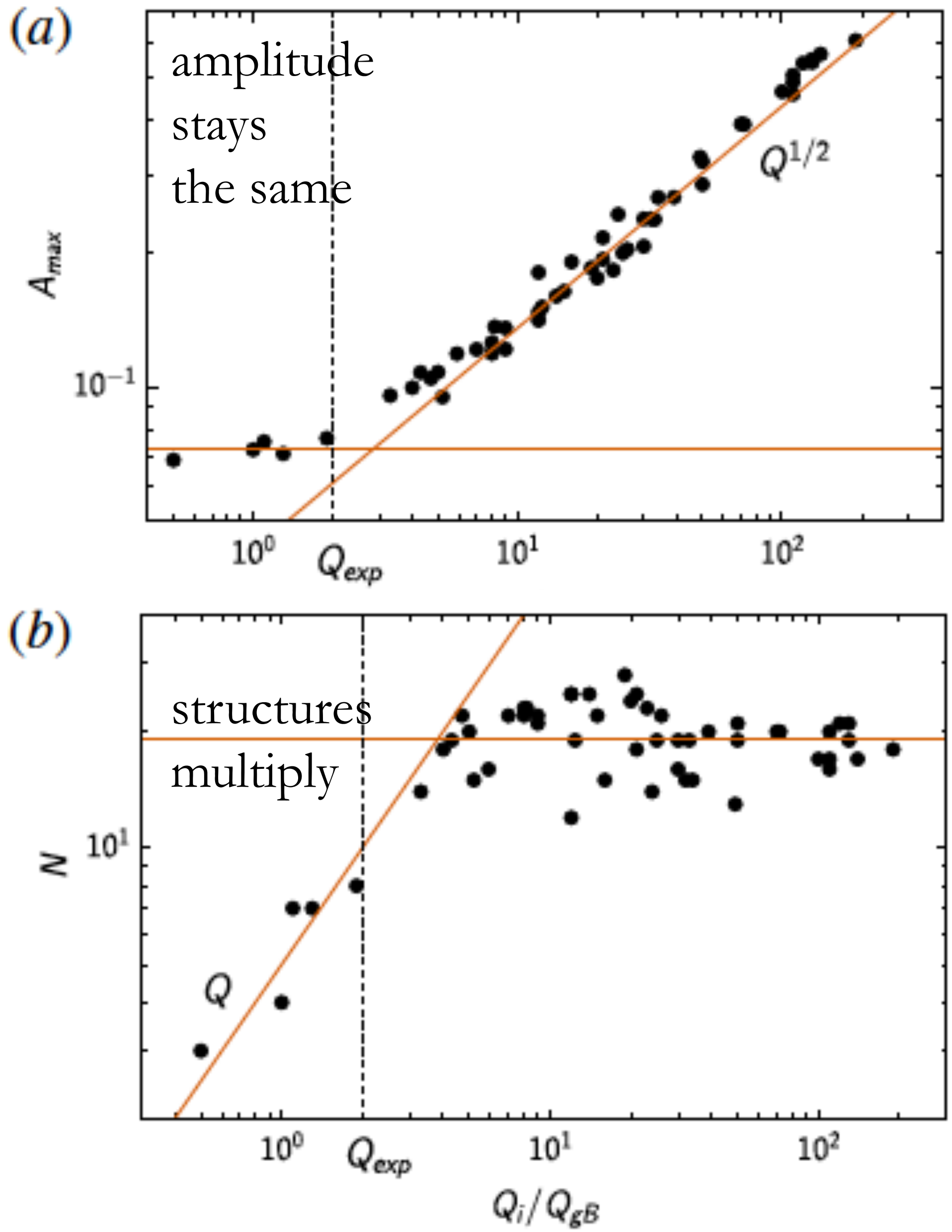

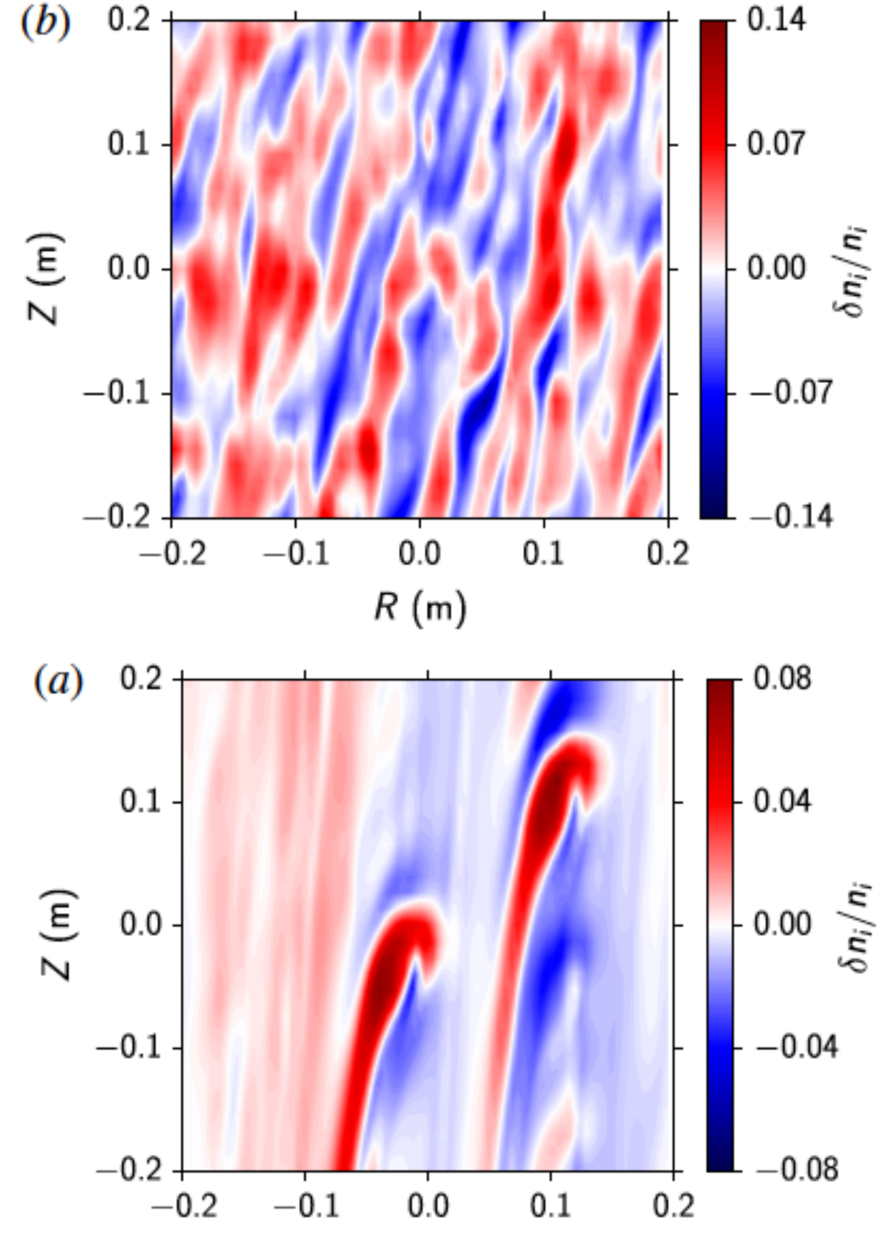

F. van Wyk et al. 2016, JPP 82, 905820609

Transition by Structure Multiplication

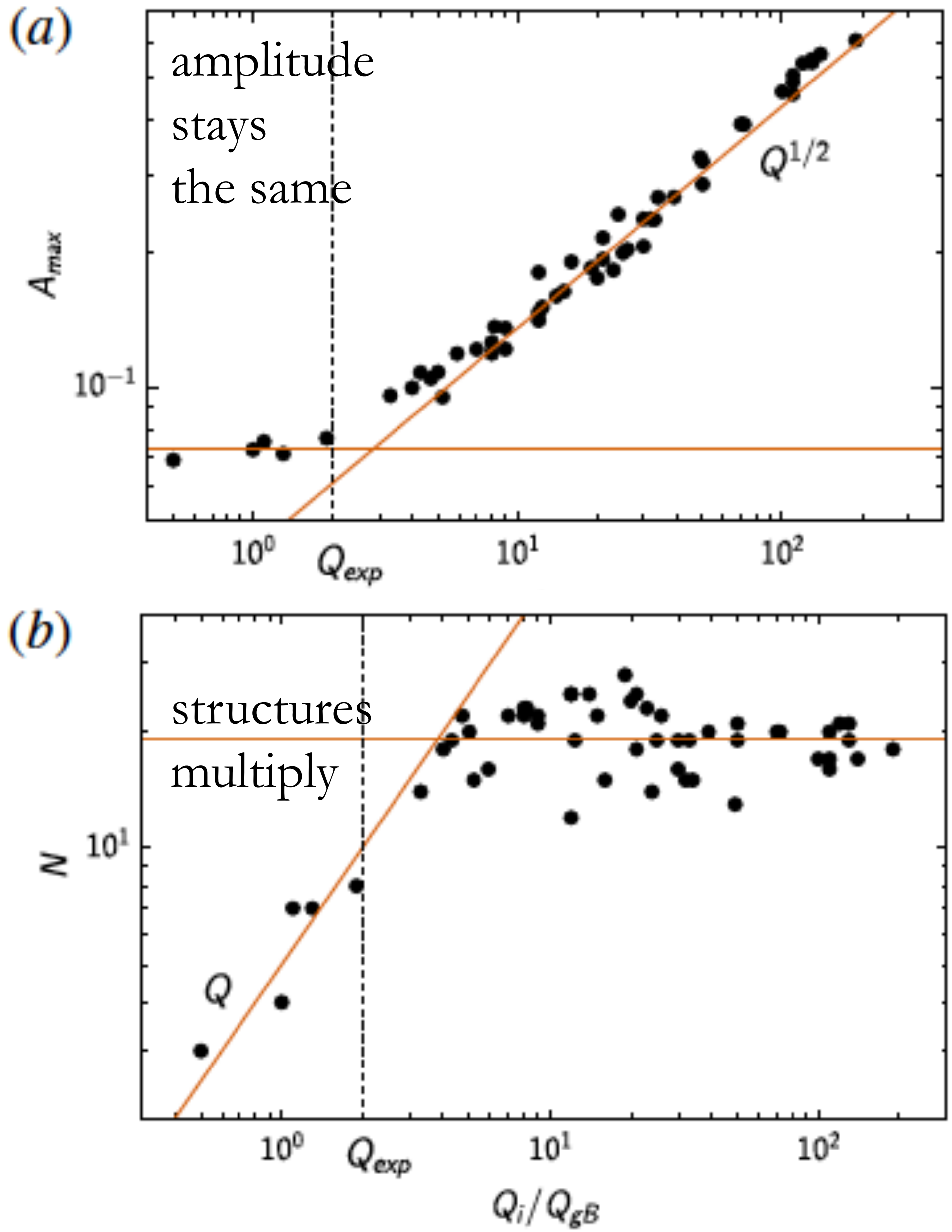

$$\frac{Q_i}{Q_{\rm gB}} \sim \frac{a}{\rho_i^2}\frac{\delta T_i}{T_i}\frac{v_{Er}}{v_{\rm thi}} \sim k_y\rho_i\left(\frac{a}{\rho_i}\frac{\delta n_i}{n_i}\right)^2$$

$$\sim A^2 N$$

Amplitude cannot decrease arbitrarily in a subcritical state, so turbulence makes flux small by not filling the volume

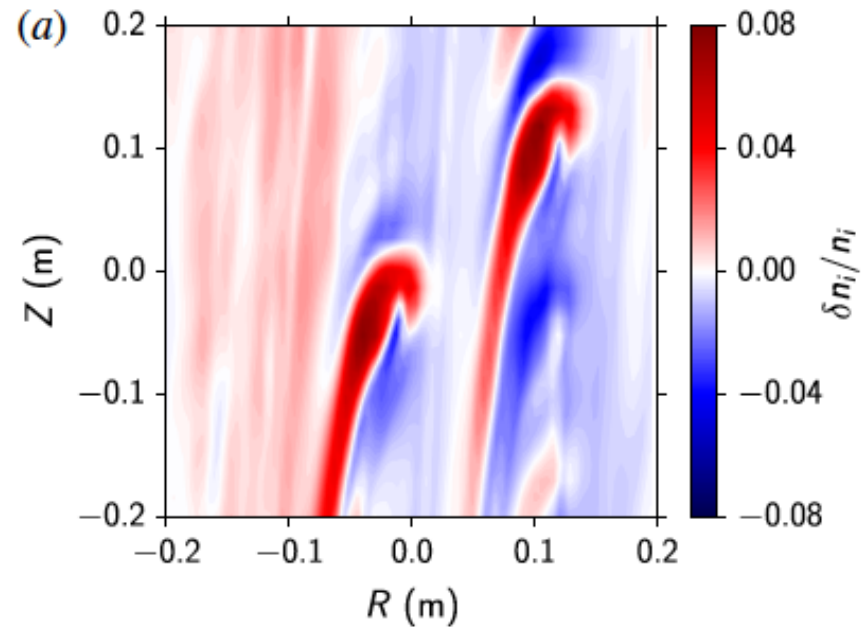

F. van Wyk et al. 2016, JPP 82, 905820609

Away From Threshold: Zonal Flows Take Over

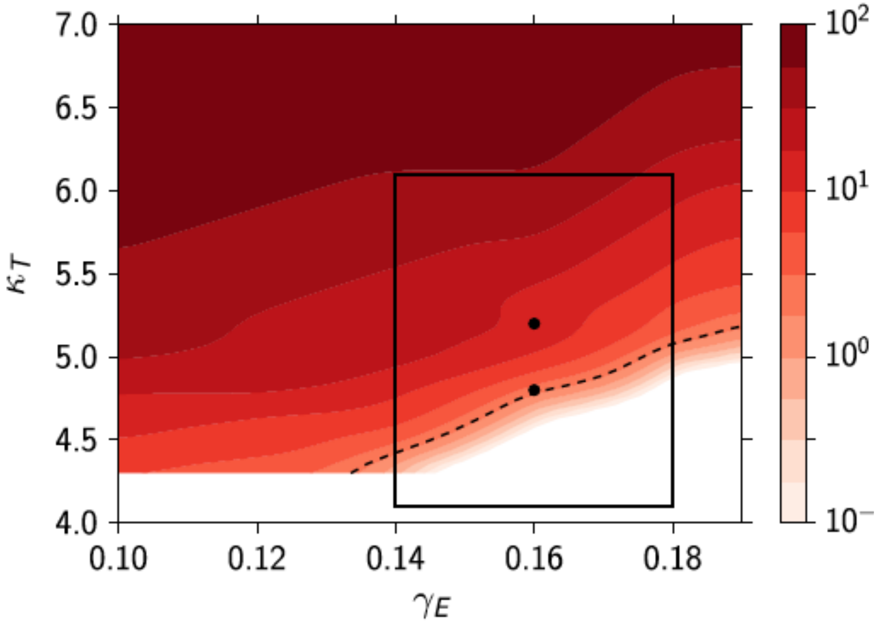

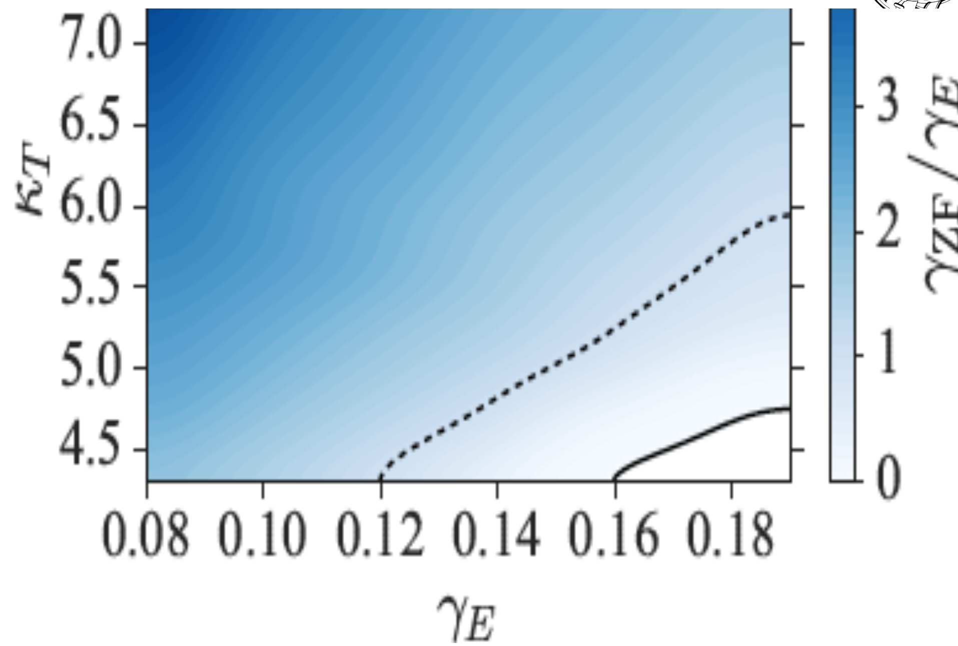

In the **structure-dominated state**, equilibrium shear dominates over zonal shear;
in the more **conventional state** away from threshold, zonal flows provide dominant shear.

<u>Experiment is in between</u>.

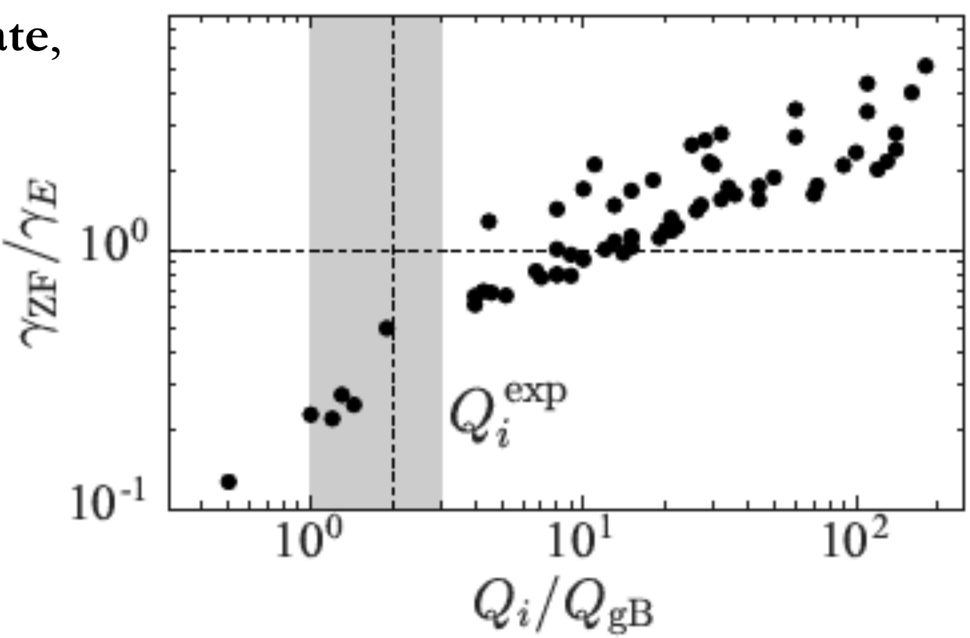

F. Van Wyk et al. 2017, PPCF 59, 114003

Smoking Gun: Symmetry Breaking

M. F. J. Fox et al. 2017, PPCF 59, 034002

MAST:

$\kappa_T = 3.1/3.3$

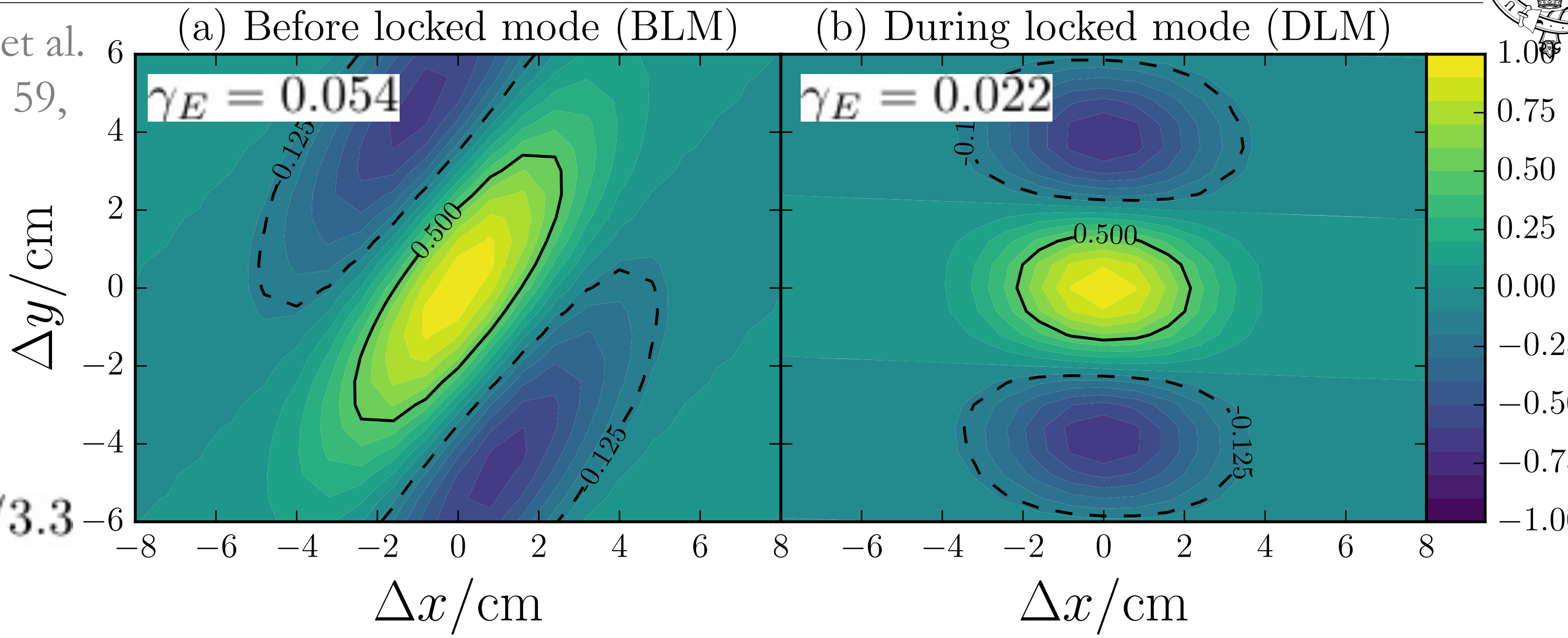

Shear breaks reflectional/up-down symmetry [Parra et al. 2011, PoP 18, 062501] of the fluctuation field.

$$(x, y, z, v_\parallel) \to (-x, y, -z, -v_\parallel)$$
$$(h, \varphi, A_\parallel, \delta B_\parallel) \to (-h, -\varphi, A_\parallel, -\delta B_\parallel)$$

In a two-point correlation function, this symmetry breaking manifests as a **tilt**.

Smoking Gun: Symmetry Breaking

M. F. J. Fox et al. 2017, PPCF 59, 034002

MAST:

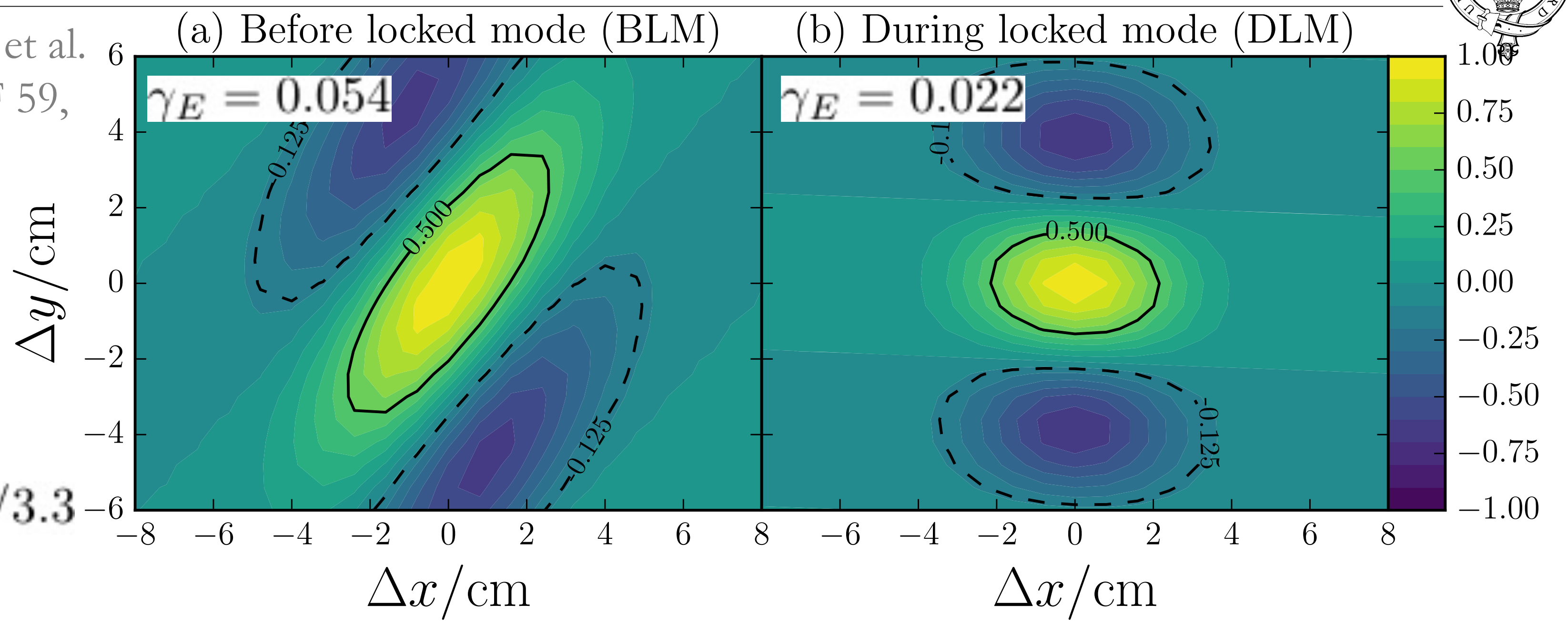

$\kappa_T = 3.1/3.3$

GS2: (not the same shot)

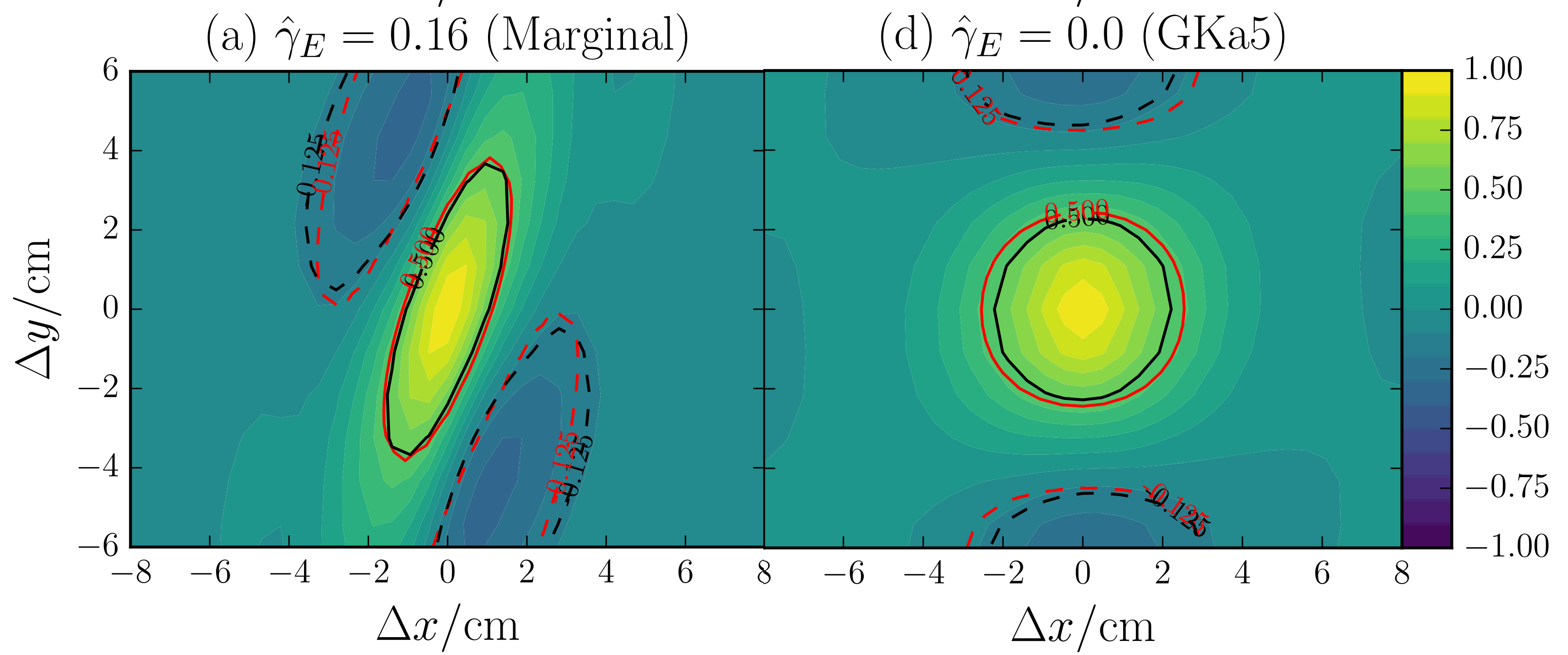

$\kappa_T = 5.1$

Smoking Gun: Symmetry Breaking

M. F. J. Fox et al. 2017, PPCF 59, 034002

The reflectional/up-down symmetry breaking
also allows the fluctuation field's one-point distribution function
to become **skewed**.
Simulations show that it indeed does so close to threshold.

This is not hard to measure experimentally!

GS2:
(not the same shot)

$\kappa_T = 5.1$

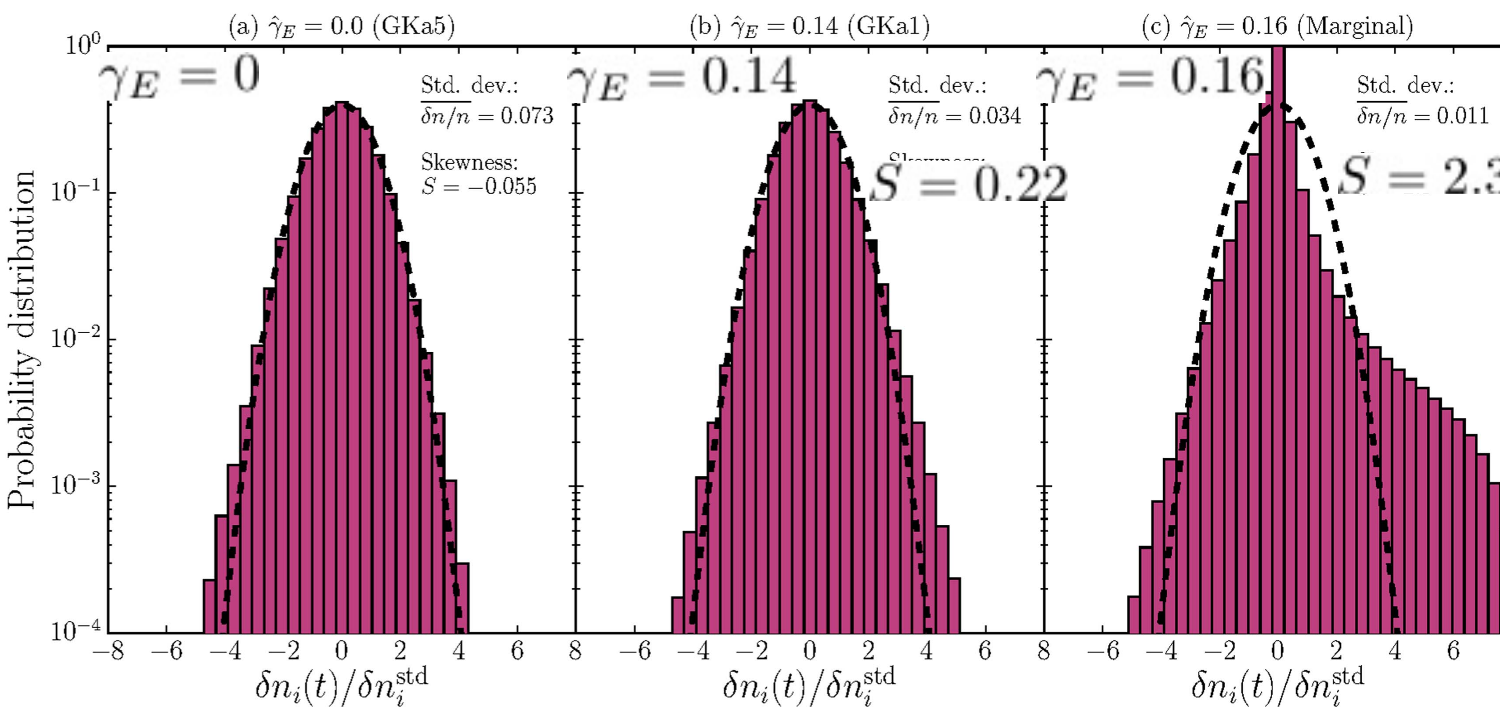

Smoking Gun: Symmetry Breaking

M. F. J. Fox et al. 2017, PPCF 59, 034002

MAST:

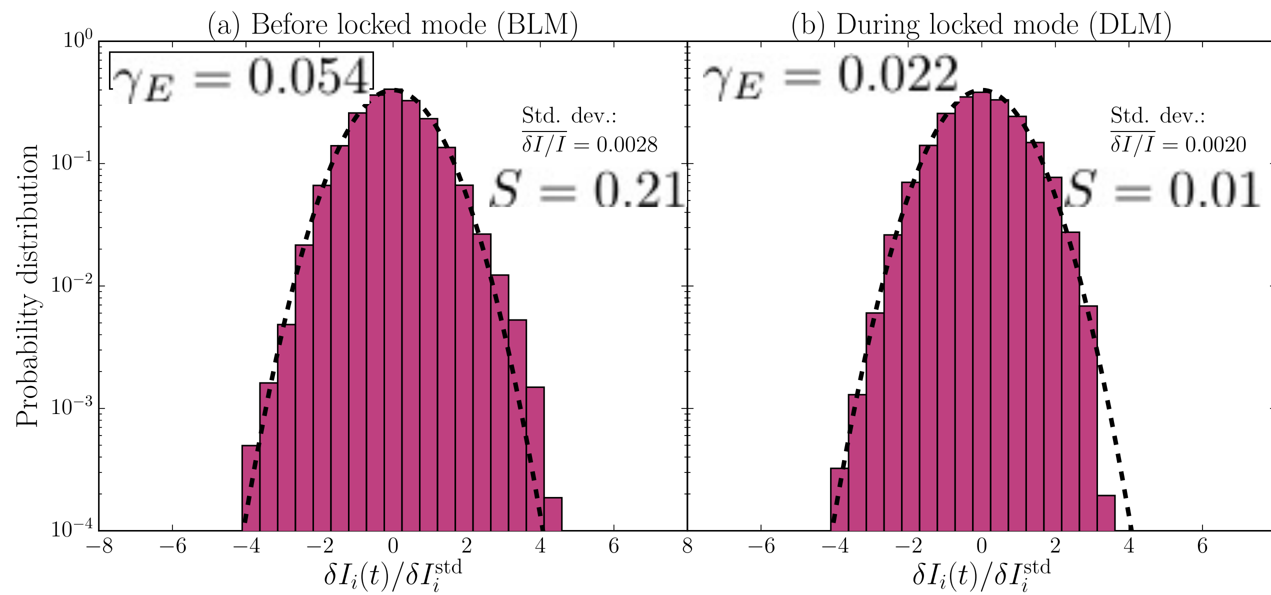

$\kappa_T = 3.1/3.3$

GS2:
(not the same shot)

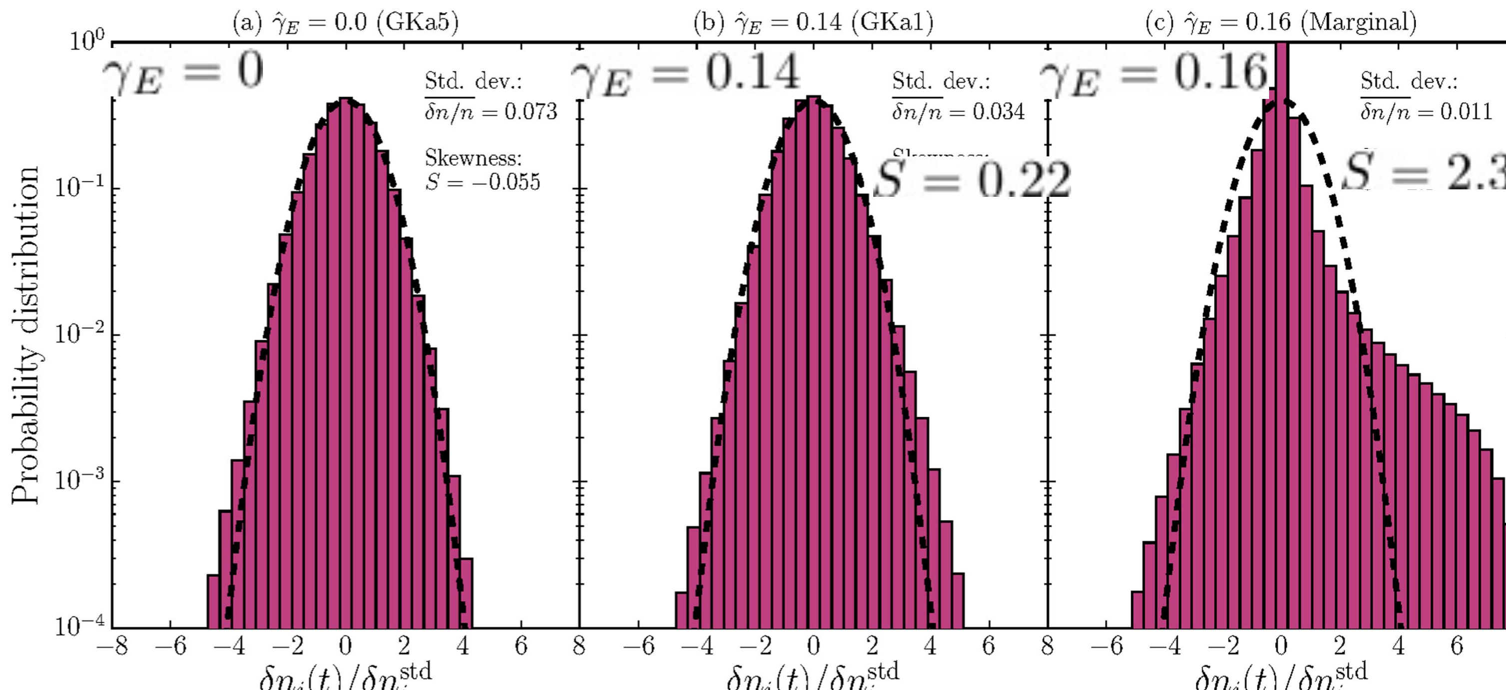

$\kappa_T = 5.1$

Restoration of Symmetry

Tilt angle: Θ/deg

a/L_{T_i}							
8.0	-2.1	25	30		42	48	47
7.0	0.86	25	36		45	47	54
6.0	-11	32	43		50	54	64
5.2	1.6	32	39	44	53	62	67
5.1					53	63	72
5.0	-3.1				55	64	
4.9	-1.4	33	39	49	60	65	
4.8	1.5	35	44	44	59	69	
4.7					60		
4.6					62		
4.5					64		
4.4	-5.2	22	46	56	69		
4.3		42	48				
$\hat{\gamma}_E$	0.00	0.08	0.10	0.12	0.14	0.16	0.18

Skewness

a/L_{T_i}							
8.0	-0.023	0.053	0.055		0.076	0.12	0.12
7.0	0.014	0.054	0.062		0.069	0.094	0.13
6.0	-0.028	0.073	0.069		0.057	0.075	0.16
5.2	-0.029	0.0100	0.048	0.045	-0.010	0.24	0.46
5.1					-0.033	0.28	3.6
5.0	0.0065				-0.039	0.40	
4.9	-0.0075	0.057	0.011	-0.030	0.18	0.50	
4.8	-0.055	0.0057	0.097	0.053	0.22	2.3	
4.7					0.34		
4.6					0.39		
4.5					0.65		
4.4	0.026	0.011	0.15	0.061	2.0		
4.3		0.10	0.23				
$\hat{\gamma}_E$	0.00	0.08	0.10	0.12	0.14	0.16	0.18

Far from the threshold, symmetry is restored (shear no longer matters).
Tilt is more robust than skewness, presumably because it is a passive feature.

M. F. J. Fox et al. 2017, PPCF 59, 034002

Restoration of Symmetry

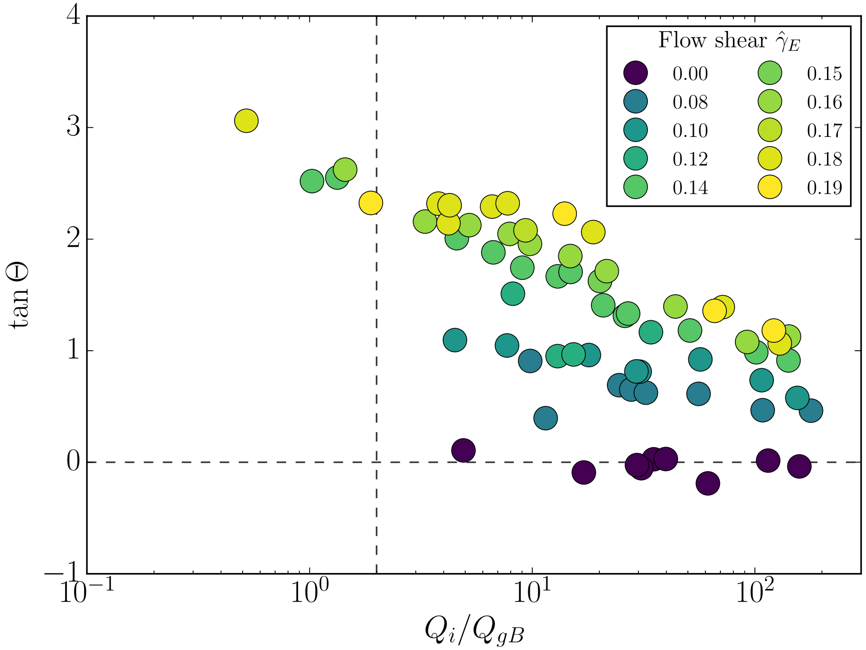

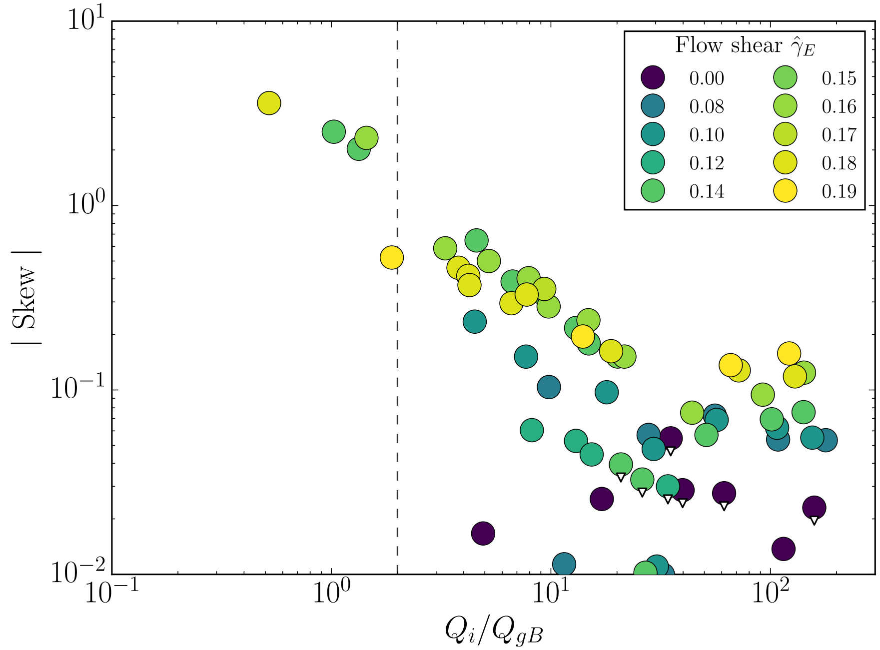

Q_i/Q_{gB} *is a good measure of distance to threshold (order parameter).*
Statistical properties depend more sensitively on it
than on individual values of the equilibrium gradients.

Far from the threshold, symmetry is restored (shear no longer matters).
Tilt is more robust than skewness, presumably because it is a passive feature.

M. F. J. Fox et al. 2017, PPCF 59, 034002

Distance to Threshold Is the Relevant Parameter

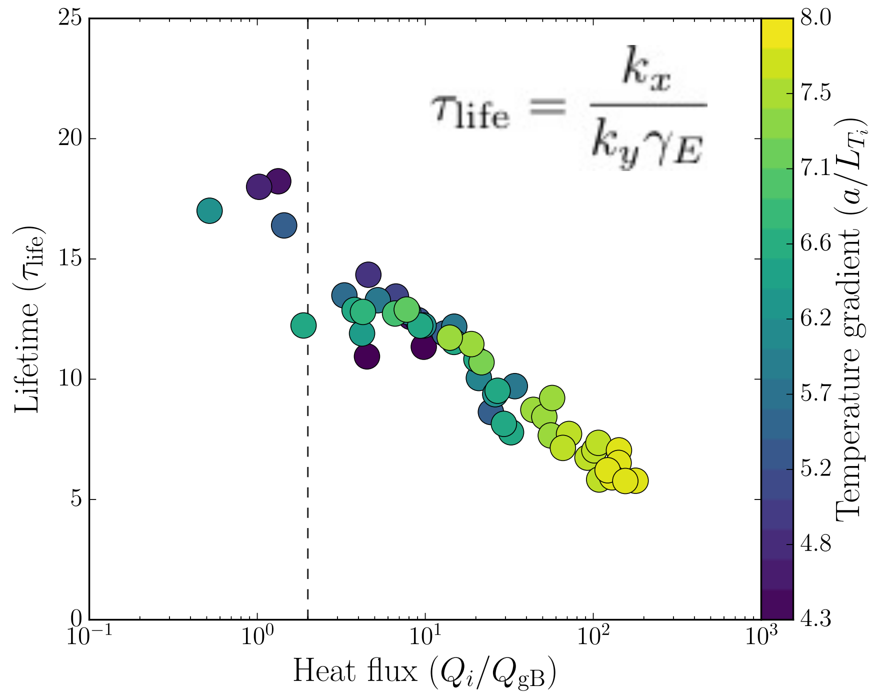

$Q_i/Q_{\rm gB}$ *is a good measure of distance to threshold (order parameter). Statistical properties depend more sensitively on it than on individual values of the equilibrium gradients.*

Far from the threshold, symmetry is restored (shear no longer matters).
Tilt is more robust than skewness, presumably because it is a passive feature.

M. F. J. Fox et al. 2017, PPCF 59, 034002

Distance to Threshold Is the Relevant Parameter

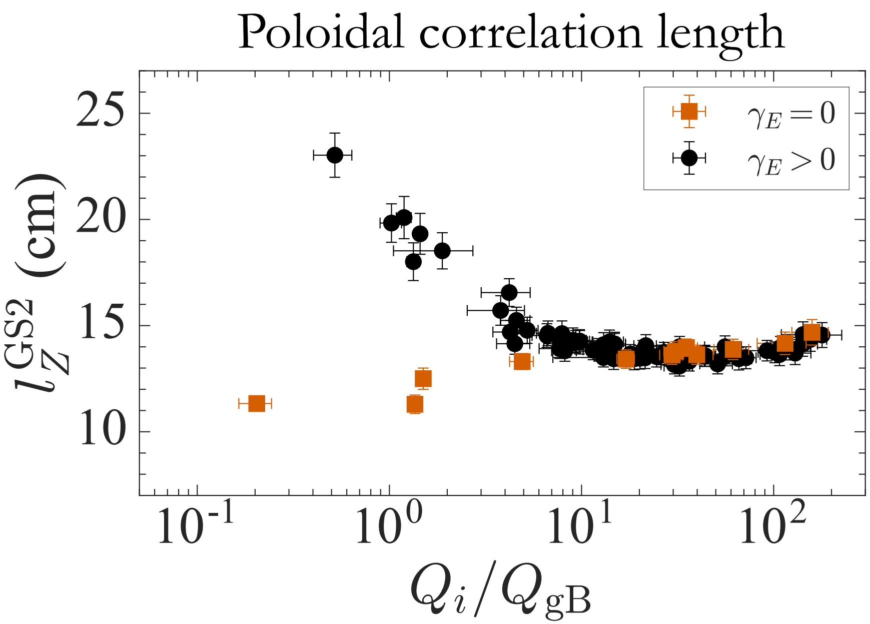

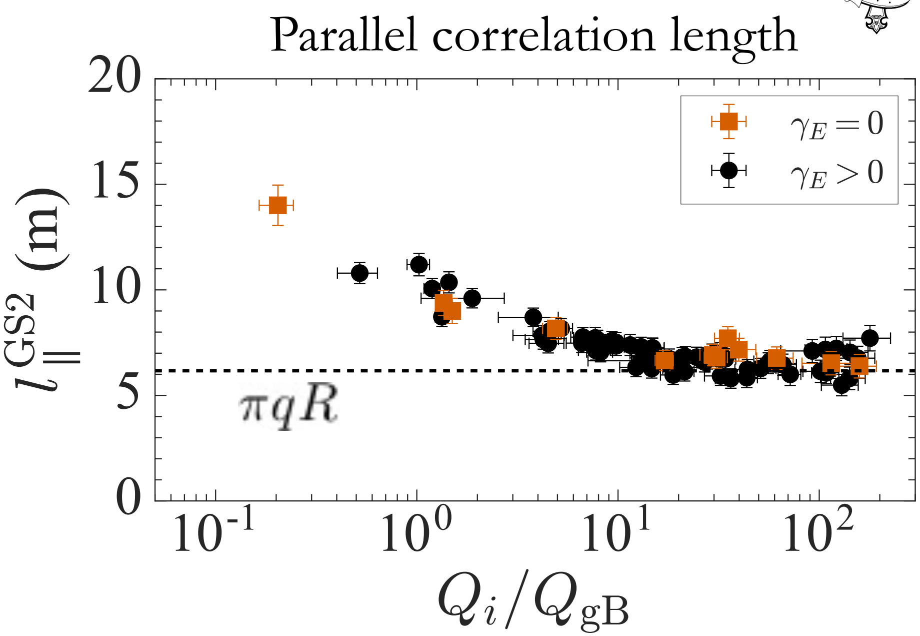

Q_i/Q_{gB} *is a good measure of distance to threshold (order parameter). Statistical properties depend more sensitively on it than on individual values of the equilibrium gradients.*

Far from the threshold, symmetry is restored (shear no longer matters).
Tilt is more robust than skewness, presumably because it is a passive feature.

F. Van Wyk et al. 2017, PPCF 59, 114003

Meanwhile, at Electron Scales…

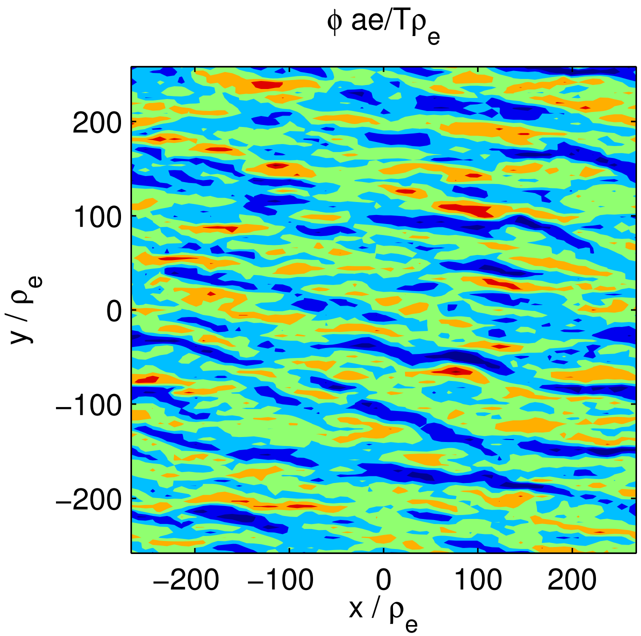

Familiar ETG “streamery” state…

<u>Standard numerical set up</u> (with GS2):

electrostatic GK,
Boltzmann ions,
collisions on,
MAST-relevant local equilibrium

G. J. Colyer et al. 2017, PPCF 59, 055002

Meanwhile, at Electron Scales…

Familiar ETG “streamery” state…

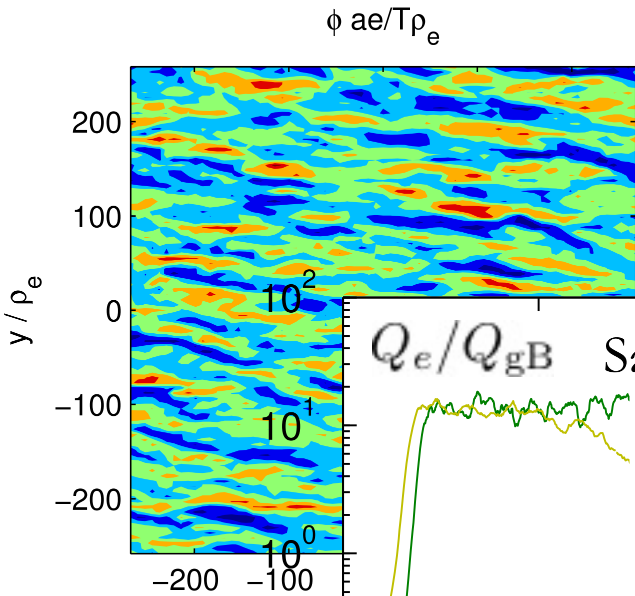

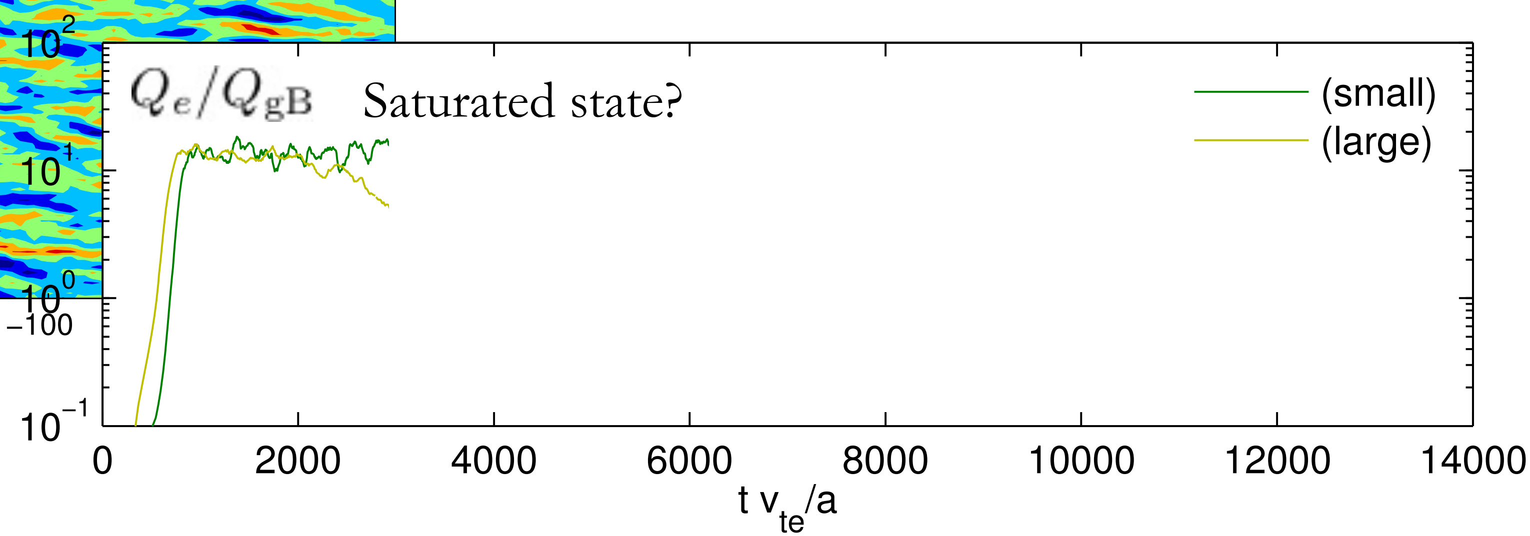

Standard numerical set up (with GS2):

electrostatic GK,
Boltzmann ions,
collisions on,
MAST-relevant local equilibrium

G. J. Colyer et al. 2017, PPCF 59, 055002

What Happens If You Wait Long Enough

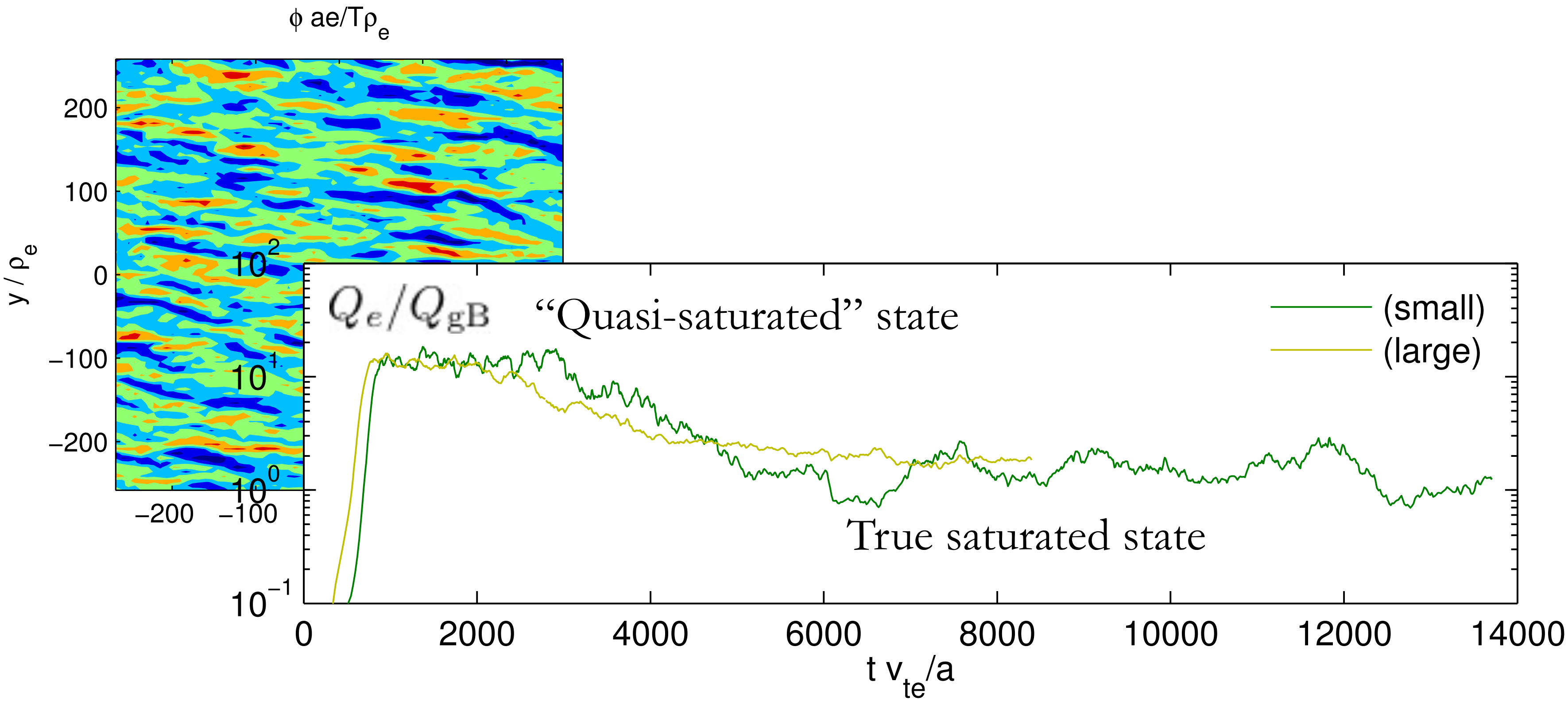

Standard numerical set up (with GS2):

electrostatic GK,

Boltzmann ions,

collisions on,

MAST-relevant local equilibrium

G. J. Colyer et al. 2017, PPCF 59, 055002

What Happens If You Wait Long Enough

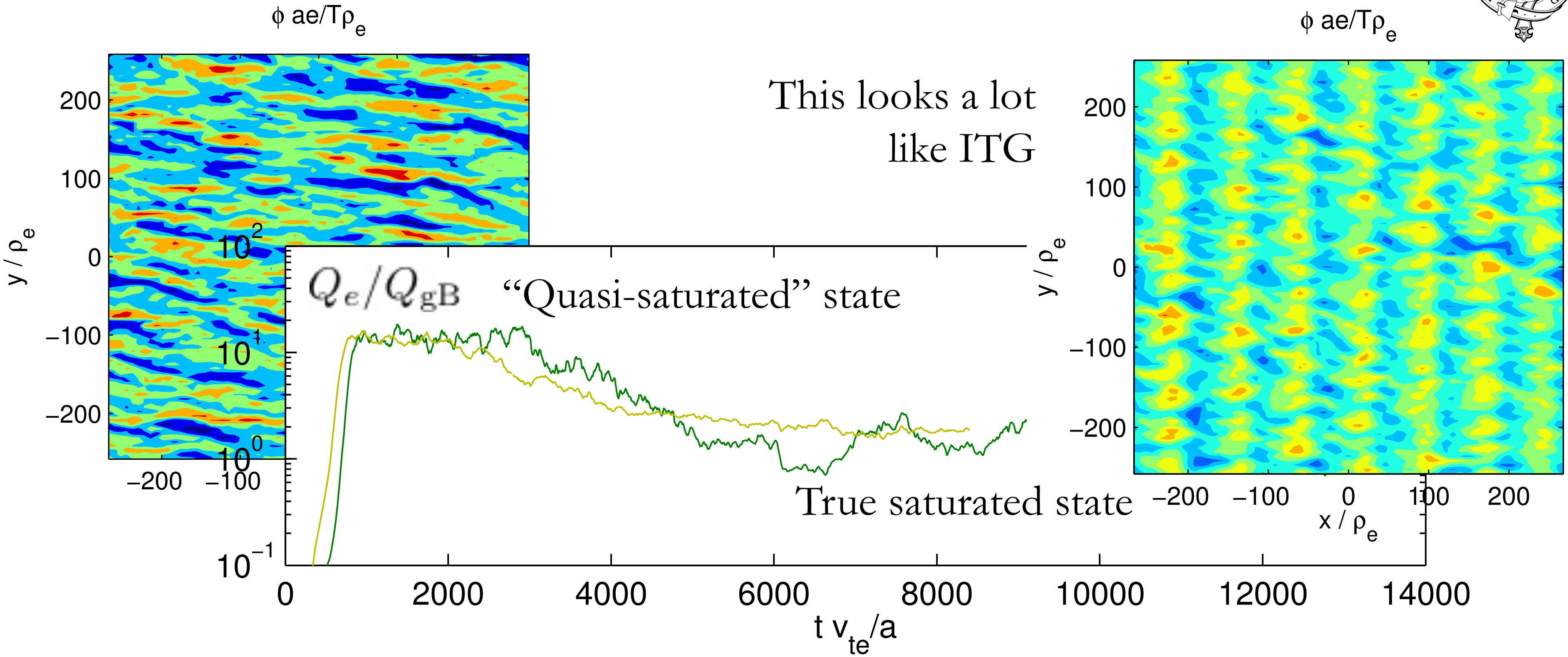

<u>Standard numerical set up</u> (with GS2):

electrostatic GK,
Boltzmann ions,
collisions on,
MAST-relevant local equilibrium

G. J. Colyer et al. 2017, PPCF 59, 055002

Zonal Flows Strike Again

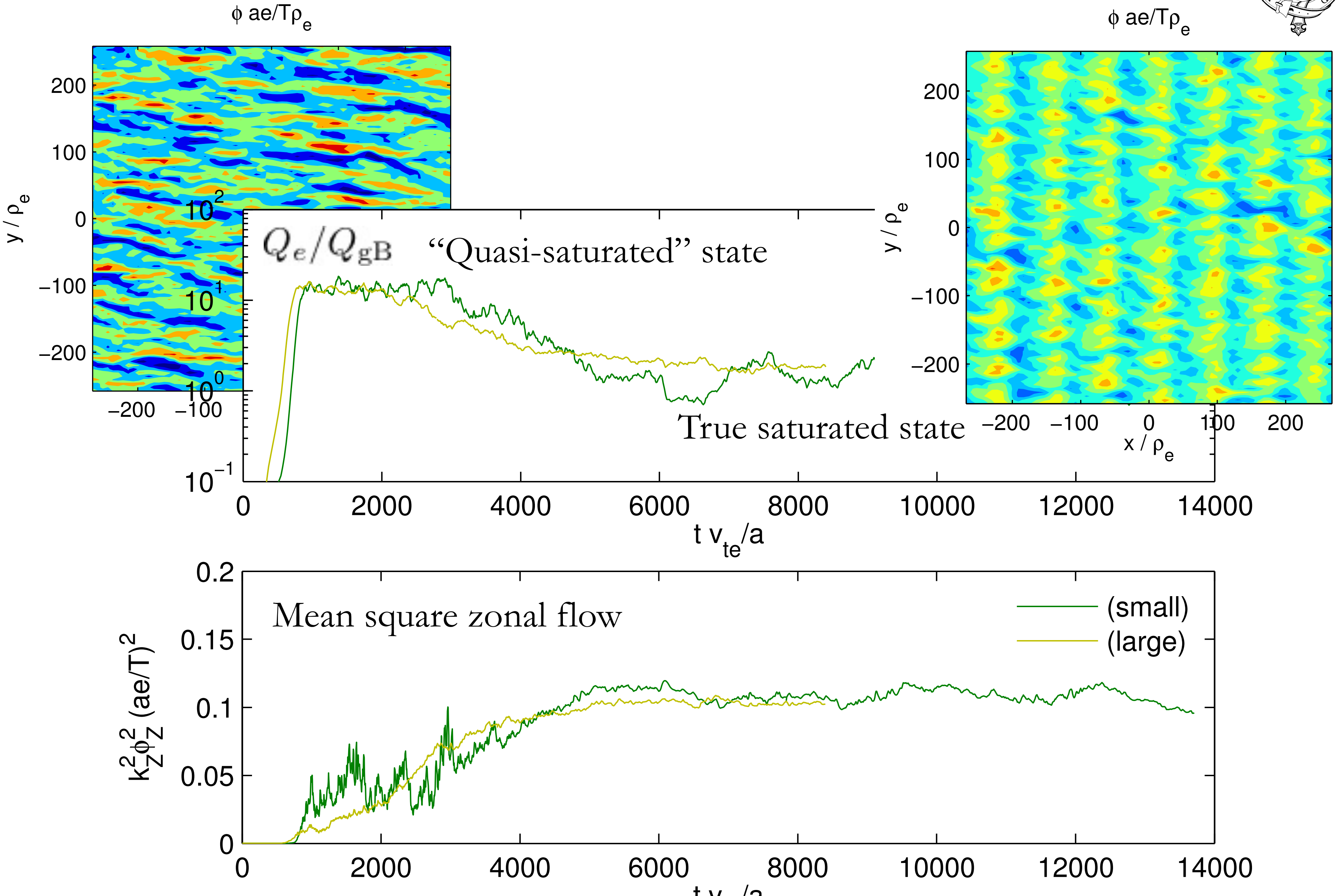

G. J. Colyer et al. 2017, PPCF 59, 055002

Zonal Flows Strike Again

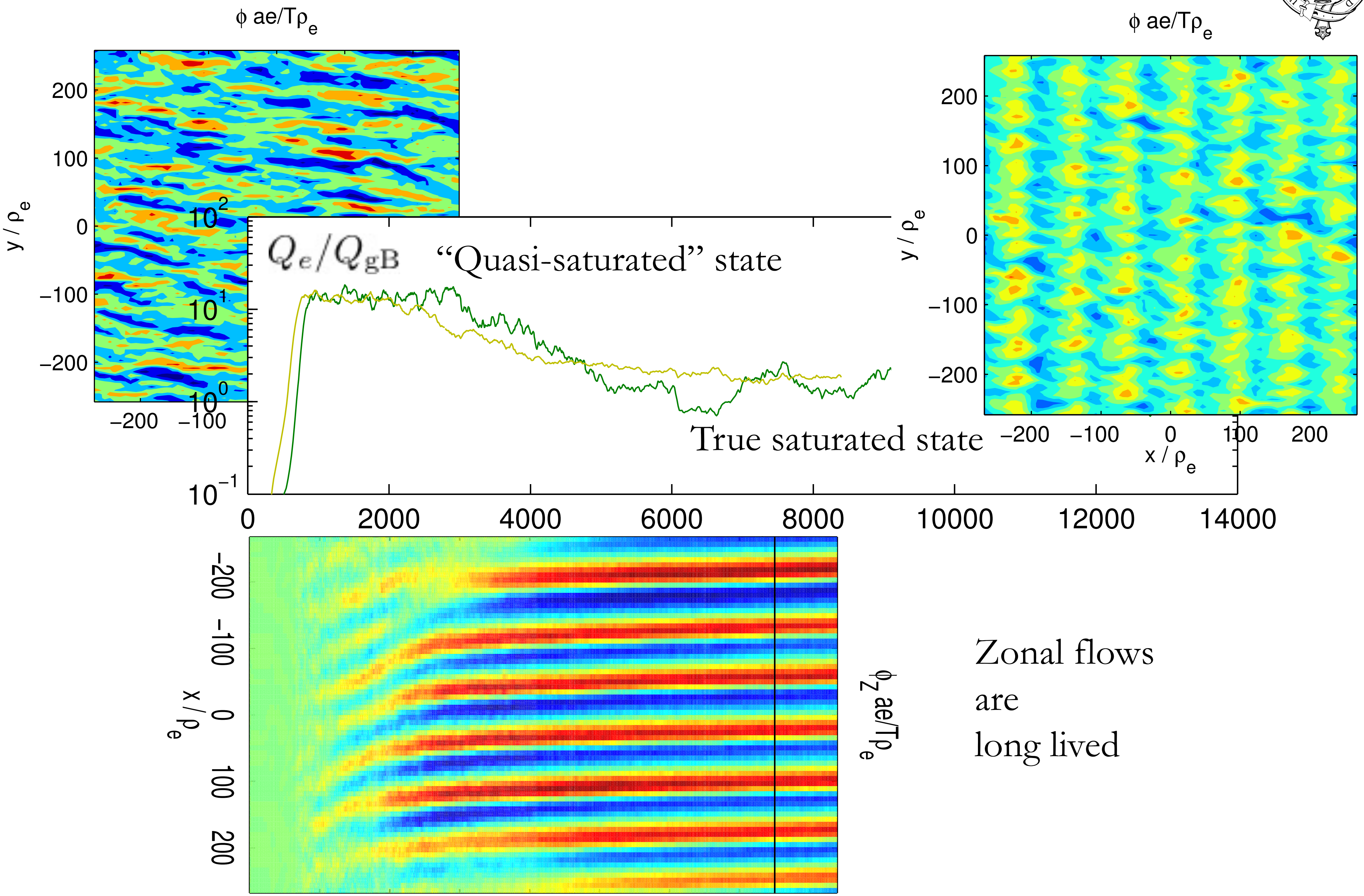

Zonal flows
are
long lived

G. J. Colyer et al. 2017, PPCF 59, 055002

Zonal Flows Strike Again

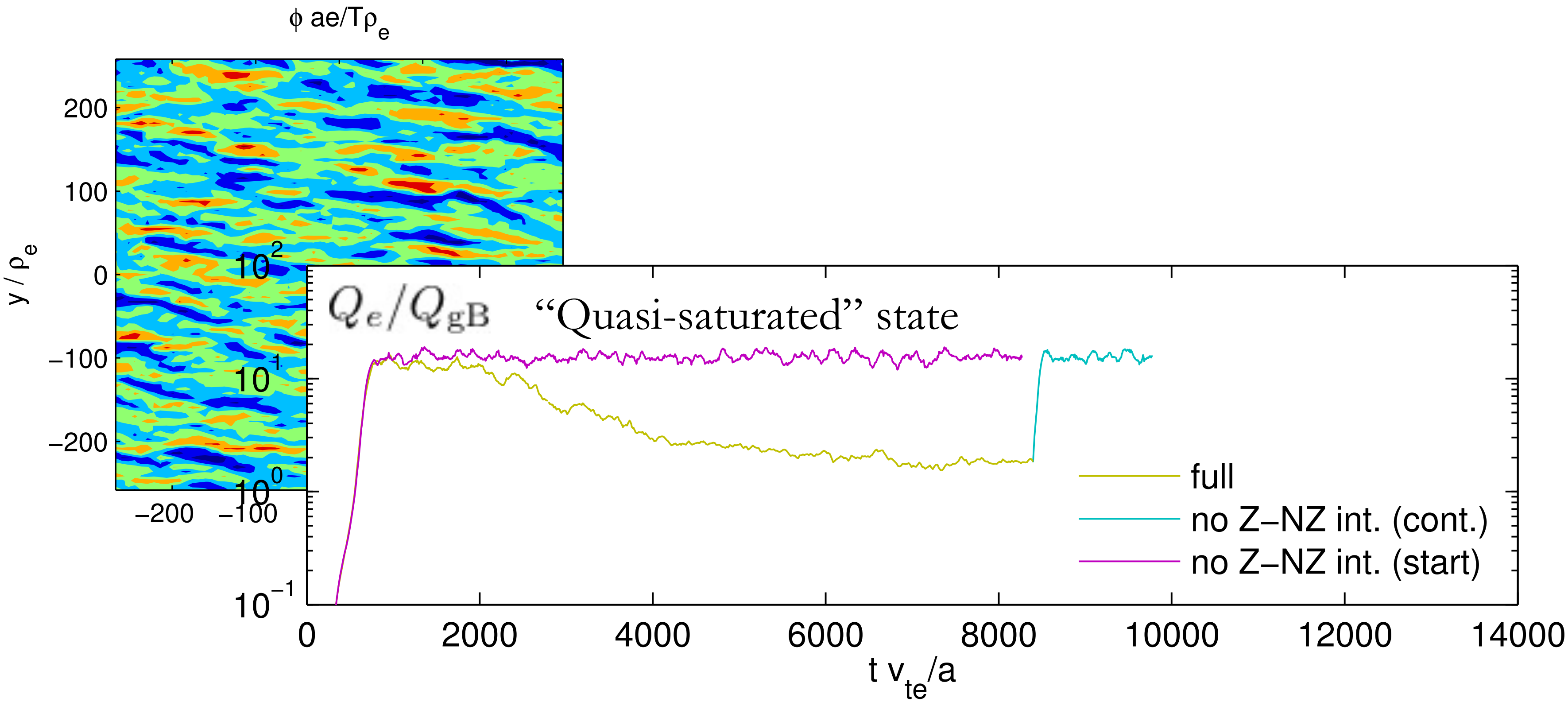

Disconnecting zonal feedback on drift waves returns the system to the “quasi-saturated” streamery state

G. J. Colyer et al. 2017, PPCF 59, 055002

Collisions Now Matter

(in the "quasi-saturated" state, heat flux did not depend on collisionality)

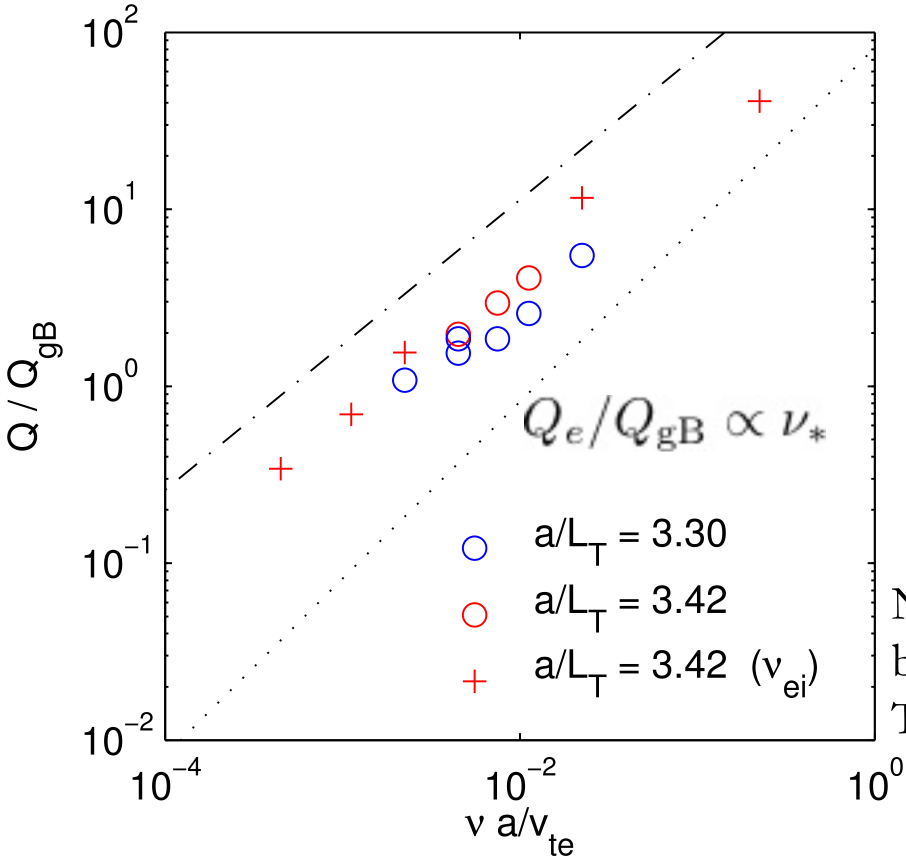

Note: crosses are obtained by varying only ν_{ei}.
This will make sense in a moment.

G. J. Colyer et al. 2017, PPCF 59, 055002

Collisions Now Matter

(in the "quasi-saturated" state, heat flux did not depend on collisionality)

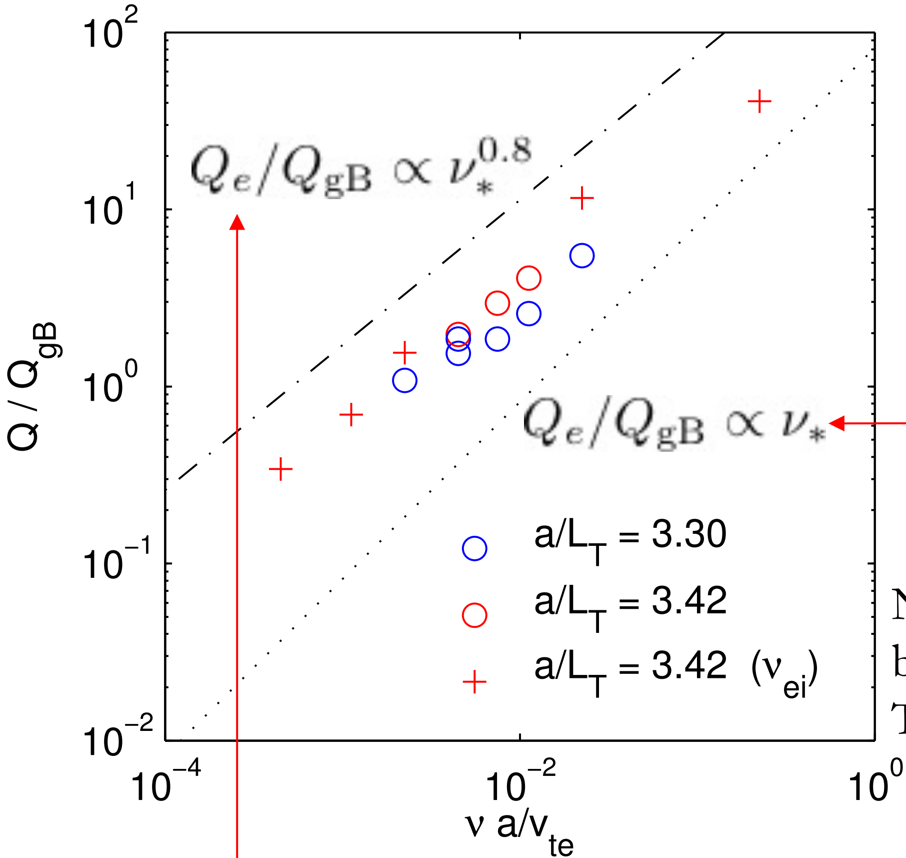

We will show that this makes sense theoretically

Note: crosses are obtained by varying only ν_{ei}. This will make sense in a moment.

MAST claims [Valovic et al. 2011, NF 51, 073045] that

$$\frac{Q}{Q_{\rm gB}} = \frac{Q}{nTv_{\rm the}\rho_*^2} = \frac{Q}{nTa\Omega_e\rho_*^3} \sim \frac{1}{\Omega_e\tau_{\rm E}\rho_*^3} \propto \frac{1}{B\tau_{\rm E}} \propto \nu_*^{0.82\pm0.1}$$

G. J. Colyer et al. 2017, PPCF 59, 055002

Zonal Modes Are Slow

$$\frac{\partial}{\partial t}\frac{e\phi}{T} = \nu_{ei} k_x^2 \rho_{pe}^2 \left(a_{11}\frac{e\phi}{T} + a_{12}\frac{\delta T}{T} \right)$$

$$\frac{\partial}{\partial t}\frac{\delta T}{T} = \nu_{ei} k_x^2 \rho_{pe}^2 \left(a_{21}\frac{e\phi}{T} + a_{22}\frac{\delta T}{T} \right) + \nu_{ee} k_x^2 \rho_{pe}^2 \left(b_{21}\frac{e\phi}{T} + b_{22}\frac{\delta T}{T} \right)$$

$$\Downarrow$$

$$\boxed{\gamma_{\mathrm{Z}} \propto \nu_{ei} k_x^2 \rho_{\mathrm{pe}}^2}$$

So it takes a while to develop zonal modes and it is hard to get rid of them.

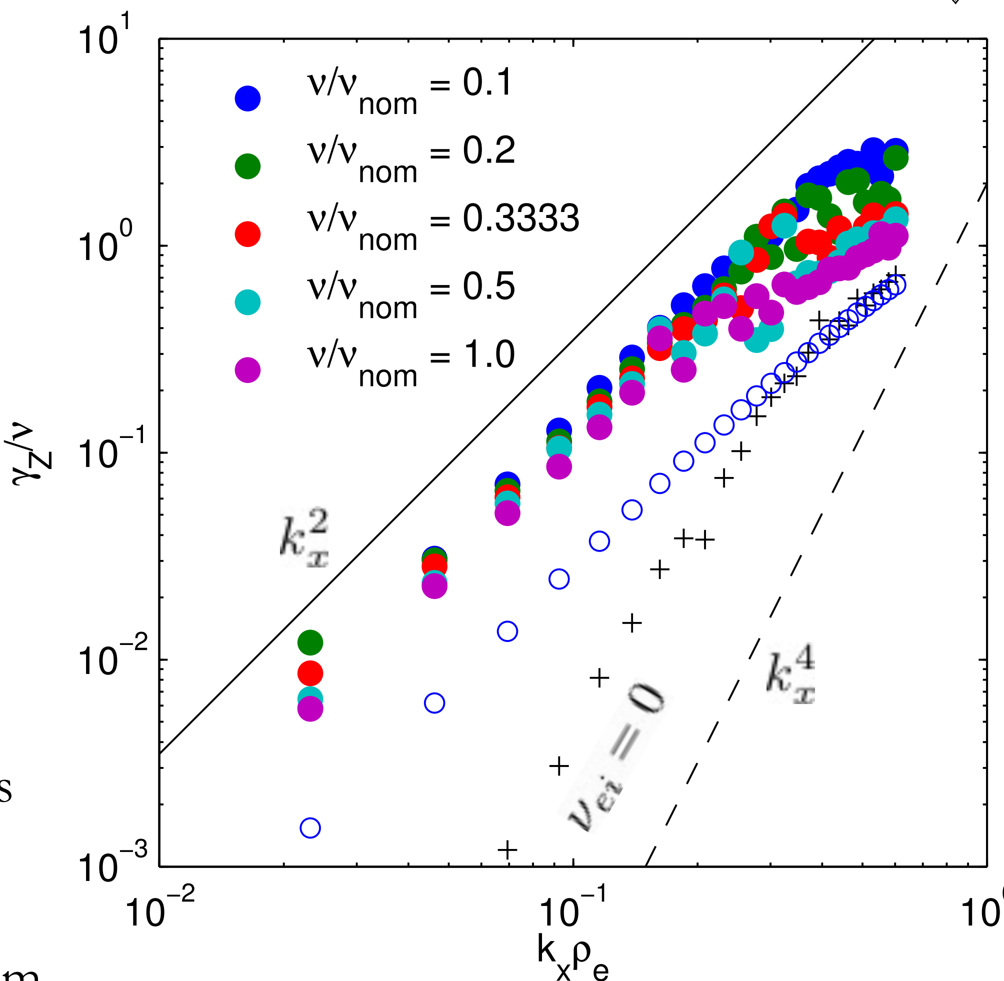

Hence the second timescale in the problem and hence also collisionality dependence (only *e-i* collisionality entering the zonal part of GK equation matters)

Note: we have verified numerically that only the zonal *e-i* collisionality affects the scaling of the heat flux

G. J. Colyer et al. 2017, PPCF 59, 055002

Zonal Modes vs. Drift Waves Détente

$$h = \underbrace{h_{\mathrm{NZ}}}_{\text{nonzonal}} + \underbrace{h_{\mathrm{Z}}}_{\text{zonal}}, \qquad \phi = \phi_{\mathrm{NZ}} + \phi_{\mathrm{Z}}$$

ELECTRON GYROKINETICS

$$\frac{\partial}{\partial t}\left(h + \frac{e\langle\phi\rangle}{T}F\right) + (\underbrace{v_{\parallel}\mathbf{b}}_{\text{streaming}} + \underbrace{\mathbf{v}_B}_{\text{mag. drifts}}) \cdot \nabla h$$

This is $\langle \delta f_e \rangle$

$$+ \underbrace{\langle \mathbf{v}_E \rangle \cdot \nabla h}_{\text{nonlinearity}} + \underbrace{\langle \mathbf{v}_E \rangle \cdot \nabla F}_{\text{drive (eq. grads)}} = \underbrace{\langle C[h] \rangle}_{\text{collisions}}$$

$$\mathbf{v}_E = \frac{c}{B}\mathbf{b} \times \nabla\phi$$

$$\underbrace{\frac{e\phi}{T_e}\left(1 + \frac{1}{\tau}\right)}_{\text{Boltzmann ions}} = -\frac{1}{n}\int \mathrm{d}^3\mathbf{v}\, \langle h \rangle_{\mathbf{r}}$$

G. J. Colyer et al. 2017, PPCF 59, 055002

Zonal Modes vs. Drift Waves Détente

$$h = \underbrace{h_{\mathrm{NZ}}}_{\text{nonzonal}} + \underbrace{h_{\mathrm{Z}}}_{\text{zonal}}, \qquad \phi = \phi_{\mathrm{NZ}} + \phi_{\mathrm{Z}}$$

$$\frac{\partial}{\partial t}\left(h_{\mathrm{NZ}} + \frac{e\langle\phi_{\mathrm{NZ}}\rangle}{T}F\right) + (v_{\|}\mathbf{b} + \mathbf{v}_B)\cdot\nabla h_{\mathrm{NZ}} - \langle C[h_{\mathrm{NZ}}]\rangle$$
$$+ \underbrace{\langle\mathbf{v}_{E,\mathrm{NZ}}\rangle\cdot\nabla h_{\mathrm{Z}} + \langle\mathbf{v}_{E,\mathrm{Z}}\rangle\cdot\nabla h_{\mathrm{NZ}}}_{\mathrm{Z-NZ\ interaction\ (I)}}$$
$$+ \langle\mathbf{v}_{E,\mathrm{NZ}}\rangle\cdot\nabla h_{\mathrm{NZ}} - \overline{\langle\mathbf{v}_{E,\mathrm{NZ}}\rangle\cdot\nabla h_{\mathrm{NZ}}} = \underbrace{-\langle\mathbf{v}_{E,\mathrm{NZ}}\rangle\cdot\nabla F}_{\mathrm{energy\ injection\ (II)}},$$

$$\frac{\partial}{\partial t}\left(h_{\mathrm{Z}} + \frac{e\langle\phi_{\mathrm{Z}}\rangle}{T}F\right) + (v_{\|}\mathbf{b} + \mathbf{v}_B)\cdot\nabla h_{\mathrm{Z}}$$
$$- \underbrace{\langle C[h_{\mathrm{Z}}]\rangle}_{\mathrm{damping\ (III)}} = \underbrace{-\overline{\langle\mathbf{v}_{E,\mathrm{NZ}}\rangle\cdot\nabla h_{\mathrm{NZ}}}}_{\mathrm{energy\ injection\ (IV)}}$$

G. J. Colyer et al. 2017, PPCF 59, 055002

Zonal Modes vs. Drift Waves Détente

$$h = \underbrace{h_{\rm NZ}}_{\text{nonzonal}} + \underbrace{h_{\rm Z}}_{\text{zonal}}, \qquad \phi = \phi_{\rm NZ} + \phi_{\rm Z} \qquad \text{NB: } \frac{h}{F} \sim \frac{e\phi}{T}$$

$$\frac{\partial}{\partial t}\left(h_{\rm NZ} + \frac{e\langle\phi_{\rm NZ}\rangle}{T}F\right) + (v_\parallel \mathbf{b} + \mathbf{v}_B)\cdot\nabla h_{\rm NZ} - \langle C[h_{\rm NZ}]\rangle$$

$$+ \underbrace{\langle \mathbf{v}_{E,{\rm NZ}}\rangle \cdot \nabla h_{\rm Z} + \langle \mathbf{v}_{E,{\rm Z}}\rangle \cdot \nabla h_{\rm NZ}}_{\text{Z–NZ interaction (I)}} \sim \frac{c}{B}k_y\phi_{\rm NZ}k_{\rm Z}h_{\rm Z}$$

$$+ \cancel{\langle \mathbf{v}_{E,{\rm NZ}}\rangle \cdot \nabla h_{\rm NZ} - \overline{\langle \mathbf{v}_{E,{\rm NZ}}\rangle \cdot \nabla h_{\rm NZ}}} = \underbrace{-\langle \mathbf{v}_{E,{\rm NZ}}\rangle \cdot \nabla F}_{\text{energy injection (II)}} \sim \frac{c}{B}k_y\phi_{\rm NZ}\frac{F}{L_T}$$

$$\frac{\partial}{\partial t}\left(h_{\rm Z} + \frac{e\langle\phi_{\rm Z}\rangle}{T}F\right) + (v_\parallel \mathbf{b} + \mathbf{v}_B)\cdot\nabla h_{\rm Z}$$

$$- \underbrace{\langle C[h_{\rm Z}]\rangle}_{\text{damping (III)}} = \underbrace{-\overline{\langle \mathbf{v}_{E,{\rm NZ}}\rangle \cdot \nabla h_{\rm NZ}}}_{\text{energy injection (IV)}}$$

$$\sim \gamma_{\rm Z}h_{\rm Z} \qquad \sim \frac{c}{B}k_{\rm Z}k_y\phi_{\rm NZ}h_{\rm NZ}$$

G. J. Colyer et al. 2017, PPCF 59, 055002

Zonal Modes vs. Drift Waves Détente

$$h = \underbrace{h_{\rm NZ}}_{\text{nonzonal}} + \underbrace{h_{\rm Z}}_{\text{zonal}}, \qquad \phi = \phi_{\rm NZ} + \phi_{\rm Z} \qquad \text{NB: } \frac{h}{F} \sim \frac{e\phi}{T}$$

$$k_{\rm Z} h_{\rm Z} \sim \frac{F}{L_T}$$

$$\frac{c}{B} k_y \phi_{\rm NZ} k_{\rm Z} h_{\rm Z}$$

Note: this argument is unlikely
to be valid far from threshold:
presumably, NZ-NZ interactions
will start to matter
[see Barnes et al. 2011, PRL 107, 115003]

$$\frac{c}{B} k_y \phi_{\rm NZ} \frac{F}{L_T}$$

$$\frac{\partial}{\partial t}\left(h_{\rm Z} + \frac{e\langle\phi_{\rm Z}\rangle}{T} F\right) + (v_\parallel \mathbf{b} + \mathbf{v}_B)\cdot\nabla h_{\rm Z} - \underbrace{\langle C[h_{\rm Z}]\rangle}_{\text{damping (III)}} = \underbrace{-\overline{\langle \mathbf{v}_{E,\rm NZ}\rangle \cdot \nabla h_{\rm NZ}}}_{\text{energy injection (IV)}}$$

$$\sim \gamma_{\rm Z} h_{\rm Z} \qquad\qquad \sim \frac{c}{B} k_{\rm Z} k_y \phi_{\rm NZ} h_{\rm NZ}$$

G. J. Colyer et al. 2017, PPCF 59, 055002

Zonal Modes vs. Drift Waves Détente

$$h = \underbrace{h_{\rm NZ}}_{\text{nonzonal}} + \underbrace{h_{\rm Z}}_{\text{zonal}}, \quad \phi = \phi_{\rm NZ} + \phi_{\rm Z}$$

NB: $\dfrac{h}{F} \sim \dfrac{e\phi}{T}$

$$k_{\rm Z} h_{\rm Z} \sim \frac{F}{L_T}$$

$$\Downarrow$$

$$\boxed{k_{\rm Z} \frac{e\phi_{\rm Z}}{T} \sim \frac{1}{L_T}} \Leftrightarrow k_{\rm Z} \frac{\delta T}{T} \sim \frac{1}{L_T}$$

$$\frac{\partial}{\partial t}\left(h_{\rm Z} + \frac{e\langle\phi_{\rm Z}\rangle}{T}F\right) + (v_\parallel \mathbf{b} + \mathbf{v}_B)\cdot\nabla h_{\rm Z} - \underbrace{\langle C[h_{\rm Z}]\rangle}_{\text{damping (III)}} = \underbrace{-\overline{\langle \mathbf{v}_{E,\rm NZ}\rangle \cdot \nabla h_{\rm NZ}}}_{\text{energy injection (IV)}}$$

$$\sim \gamma_{\rm Z} h_{\rm Z} \qquad \sim \frac{c}{B} k_{\rm Z} k_y \phi_{\rm NZ} h_{\rm NZ}$$

G. J. Colyer et al. 2017, PPCF 59, 055002

Zonal Modes vs. Drift Waves Détente

$$h = \underbrace{h_{NZ}}_{\text{nonzonal}} + \underbrace{h_Z}_{\text{zonal}}, \qquad \phi = \phi_{NZ} + \phi_Z$$

NB: $\dfrac{h}{F} \sim \dfrac{e\phi}{T}$

$$k_Z h_Z \sim \frac{F}{L_T}$$

$$\Downarrow$$

$$\boxed{k_Z \frac{e\phi_Z}{T} \sim \frac{1}{L_T}} \Leftrightarrow k_Z \frac{\delta T}{T} \sim \frac{1}{L_T}$$

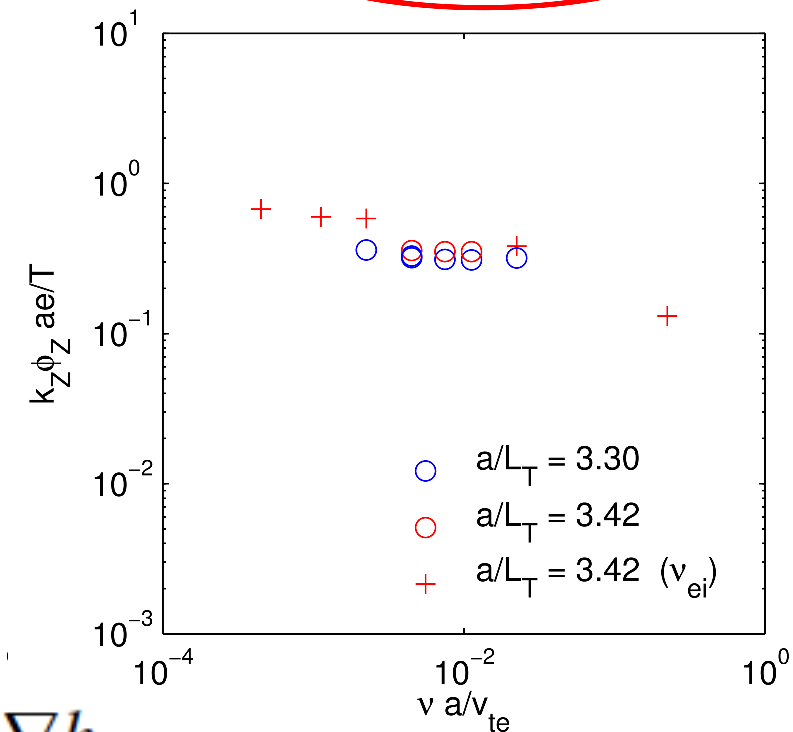

$$\frac{\partial}{\partial t}\left(h_Z + \frac{e\langle\phi_Z\rangle}{T}F\right) + (v_\parallel \mathbf{b} + \mathbf{v}_B)\cdot\nabla h_Z - \underbrace{\langle C[h_Z]\rangle}_{\text{damping (III)}} = \underbrace{-\overline{\langle \mathbf{v}_{E,NZ}\rangle \cdot \nabla h_{NZ}}}_{\text{energy injection (IV)}}$$

$$\sim \gamma_Z h_Z \qquad\qquad \sim \frac{c}{B} k_Z k_y \phi_{NZ} h_{NZ}$$

G. J. Colyer et al. 2017, PPCF 59, 055002

Zonal Modes vs. Drift Waves Détente

$$h = \underbrace{h_{\rm NZ}}_{\text{nonzonal}} + \underbrace{h_{\rm Z}}_{\text{zonal}}, \qquad \phi = \phi_{\rm NZ} + \phi_{\rm Z}$$

$$\boxed{k_{\rm Z}\frac{e\phi_{\rm Z}}{T} \sim \frac{1}{L_T}}$$

$$\frac{\phi_{\rm NZ}^2}{\phi_{\rm Z}^2} \sim \frac{\phi_{\rm NZ}h_{\rm NZ}}{\phi_{\rm Z}h_{\rm Z}} \sim \frac{\gamma_{\rm Z}B}{ck_yk_{\rm Z}\phi_{\rm Z}}$$

Note: this argument is unlikely to be valid far from threshold: presumably, zonal flows will be limited by tertiary instability, not collisional viscosity [see Rogers et al. 2000, PRL 85, 5336]

$\gamma_{\rm Z}h_{\rm Z}$ $\qquad$ $\frac{c}{B}k_{\rm Z}k_y\phi_{\rm NZ}h_{\rm NZ}$

G. J. Colyer et al. 2017, PPCF 59, 055002

Zonal Modes vs. Drift Waves Détente

$$h = \underbrace{h_{\rm NZ}}_{\text{nonzonal}} + \underbrace{h_{\rm Z}}_{\text{zonal}}, \qquad \phi = \phi_{\rm NZ} + \phi_{\rm Z}$$

$$\boxed{k_{\rm Z}\frac{e\phi_{\rm Z}}{T} \sim \frac{1}{L_T}}$$

$$\frac{\phi_{\rm NZ}^2}{\phi_{\rm Z}^2} \sim \frac{\phi_{\rm NZ}h_{\rm NZ}}{\phi_{\rm Z}h_{\rm Z}} \sim \frac{\gamma_{\rm Z}B}{ck_y k_{\rm Z}\phi_{\rm Z}} \sim \frac{\gamma_{\rm Z}eBL_T}{ck_y T} \sim \frac{1}{k_y\rho_e}\frac{\gamma_{\rm Z}}{v_{\rm the}/L_T}$$

Note: this argument is unlikely to be valid far from threshold: presumably, zonal flows will be limited by tertiary instability, not collisional viscosity [see Rogers et al. 2000, PRL 85, 5336]

$\gamma_{\rm Z}h_{\rm Z}$ $\qquad$ $\frac{c}{B}k_{\rm Z}k_y\phi_{\rm NZ}h_{\rm NZ}$

G. J. Colyer et al. 2017, PPCF 59, 055002

Zonal Modes vs. Drift Waves Détente

$$h = \underbrace{h_{\rm NZ}}_{\text{nonzonal}} + \underbrace{h_{\rm Z}}_{\text{zonal}}, \qquad \phi = \phi_{\rm NZ} + \phi_{\rm Z}$$

$$\boxed{k_{\rm Z}\frac{e\phi_{\rm Z}}{T} \sim \frac{1}{L_T}}$$

$$\boxed{\frac{\phi_{\rm NZ}^2}{\phi_{\rm Z}^2} \sim \frac{1}{k_y\rho_e}\frac{\gamma_{\rm Z}}{v_{\rm the}/L_T}}$$

$$\frac{Q}{Q_{\rm gB}} \sim \frac{n\delta T_{\rm NZ}v_{Ex}}{nTv_{\rm the}\rho_*^2} \sim \frac{\delta T_{\rm NZ}}{T}\frac{ck_y\phi_{\rm NZ}}{Bv_{\rm the}\rho_*^2} \sim k_y\rho_e\left(\frac{e\phi_{\rm NZ}}{T\rho_*}\right)^2$$

G. J. Colyer et al. 2017, PPCF 59, 055002

Zonal Modes vs. Drift Waves Détente

$$h = \underbrace{h_{\mathrm{NZ}}}_{\text{nonzonal}} + \underbrace{h_{\mathrm{Z}}}_{\text{zonal}}, \qquad \phi = \phi_{\mathrm{NZ}} + \phi_{\mathrm{Z}}$$

$$\boxed{k_{\mathrm{Z}} \frac{e\phi_{\mathrm{Z}}}{T} \sim \frac{1}{L_T}}$$

$$\boxed{\frac{\phi_{\mathrm{NZ}}^2}{\phi_{\mathrm{Z}}^2} \sim \frac{1}{k_y \rho_e} \frac{\gamma_{\mathrm{Z}}}{v_{\mathrm{th}e}/L_T}}$$

$$\frac{Q}{Q_{\mathrm{gB}}} \sim \frac{n\delta T_{\mathrm{NZ}} v_{Ex}}{nTv_{\mathrm{th}e}\rho_*^2} \sim \frac{\delta T_{\mathrm{NZ}}}{T} \frac{ck_y\phi_{\mathrm{NZ}}}{Bv_{\mathrm{th}e}\rho_*^2} \sim k_y\rho_e \left(\frac{e\phi_{\mathrm{NZ}}}{T\rho_*}\right)^2$$

$$\sim \frac{\gamma_{\mathrm{Z}}}{v_{\mathrm{th}e}/L_T} \left(\frac{e\phi_{\mathrm{Z}}}{T\rho_*}\right)^2$$

G. J. Colyer et al. 2017, PPCF 59, 055002

Zonal Modes vs. Drift Waves Détente

$$h = \underbrace{h_{\rm NZ}}_{\text{nonzonal}} + \underbrace{h_{\rm Z}}_{\text{zonal}}, \qquad \phi = \phi_{\rm NZ} + \phi_{\rm Z}$$

$$\boxed{k_{\rm Z}\frac{e\phi_{\rm Z}}{T} \sim \frac{1}{L_T}}$$

$$\frac{\phi_{\rm NZ}^2}{\phi_{\rm Z}^2} \sim \frac{1}{k_y\rho_e}\frac{\gamma_{\rm Z}}{v_{\rm the}/L_T}$$

$$\frac{Q}{Q_{\rm gB}} \sim \frac{n\delta T_{\rm NZ}v_{Ex}}{nTv_{\rm the}\rho_*^2} \sim \frac{\delta T_{\rm NZ}}{T}\frac{ck_y\phi_{\rm NZ}}{Bv_{\rm the}\rho_*^2} \sim k_y\rho_e\left(\frac{e\phi_{\rm NZ}}{T\rho_*}\right)^2$$

$$\sim \frac{\gamma_{\rm Z}}{v_{\rm the}/L_T}\left(\frac{e\phi_{\rm Z}}{T\rho_*}\right)^2 \sim \frac{\gamma_{\rm Z}/k_{\rm Z}^2\rho_e^2}{v_{\rm the}/a}\frac{a}{L_T}$$

Note that we do not need to know either k_y or $k_{\rm Z}$

G. J. Colyer et al. 2017, PPCF 59, 055002

Zonal Modes vs. Drift Waves Détente

$$h = \underbrace{h_{\rm NZ}}_{\text{nonzonal}} + \underbrace{h_{\rm Z}}_{\text{zonal}}, \qquad \phi = \phi_{\rm NZ} + \phi_{\rm Z}$$

$$\gamma_{\rm Z} \sim \nu_{ei} k_{\rm Z}^2 \rho_{\rm pe}^2$$

$$\boxed{k_{\rm Z}\frac{e\phi_{\rm Z}}{T} \sim \frac{1}{L_T}}$$

$$\frac{\phi_{\rm NZ}^2}{\phi_{\rm Z}^2} \sim \frac{1}{k_y\rho_e}\frac{\gamma_{\rm Z}}{v_{\rm the}/L_T}$$

$$\frac{Q}{Q_{\rm gB}} \sim \frac{n\delta T_{\rm NZ} v_{Ex}}{nTv_{\rm the}\rho_*^2} \sim \frac{\delta T_{\rm NZ}}{T}\frac{ck_y\phi_{\rm NZ}}{Bv_{\rm the}\rho_*^2} \sim k_y\rho_e\left(\frac{e\phi_{\rm NZ}}{T\rho_*}\right)^2$$

$$\sim \frac{\gamma_{\rm Z}}{v_{\rm the}/L_T}\left(\frac{e\phi_{\rm Z}}{T\rho_*}\right)^2 \sim \frac{\gamma_{\rm Z}/k_{\rm Z}^2\rho_e^2}{v_{\rm the}/a}\frac{a}{L_T} \sim \frac{\nu_{ei}}{v_{\rm the}/a}\left(\frac{B}{B_{\rm p}}\right)^2\frac{a}{L_T}$$

Note that we do not need to know either k_y or $k_{\rm Z}$

G. J. Colyer et al. 2017, PPCF 59, 055002

Zonal Modes vs. Drift Waves Détente

$$h = \underbrace{h_{\rm NZ}}_{\text{nonzonal}} + \underbrace{h_{\rm Z}}_{\text{zonal}}, \qquad \phi = \phi_{\rm NZ} + \phi_{\rm Z}$$

$$\gamma_{\rm Z} \sim \nu_{ei} k_{\rm Z}^2 \rho_{\rm pe}^2$$

$$k_{\rm Z} \frac{e\phi_{\rm Z}}{T} \sim \frac{1}{L_T}$$

$$\frac{\phi_{\rm NZ}^2}{\phi_{\rm Z}^2} \sim \frac{1}{k_y \rho_e} \frac{\gamma_{\rm Z}}{v_{\rm the}/L_T}$$

$$\boxed{\frac{Q}{Q_{\rm gB}} \sim \frac{\nu_{ei}}{v_{\rm the}/a} \left(\frac{B}{B_{\rm p}}\right)^2 \frac{a}{L_T}}$$

q. e. d.

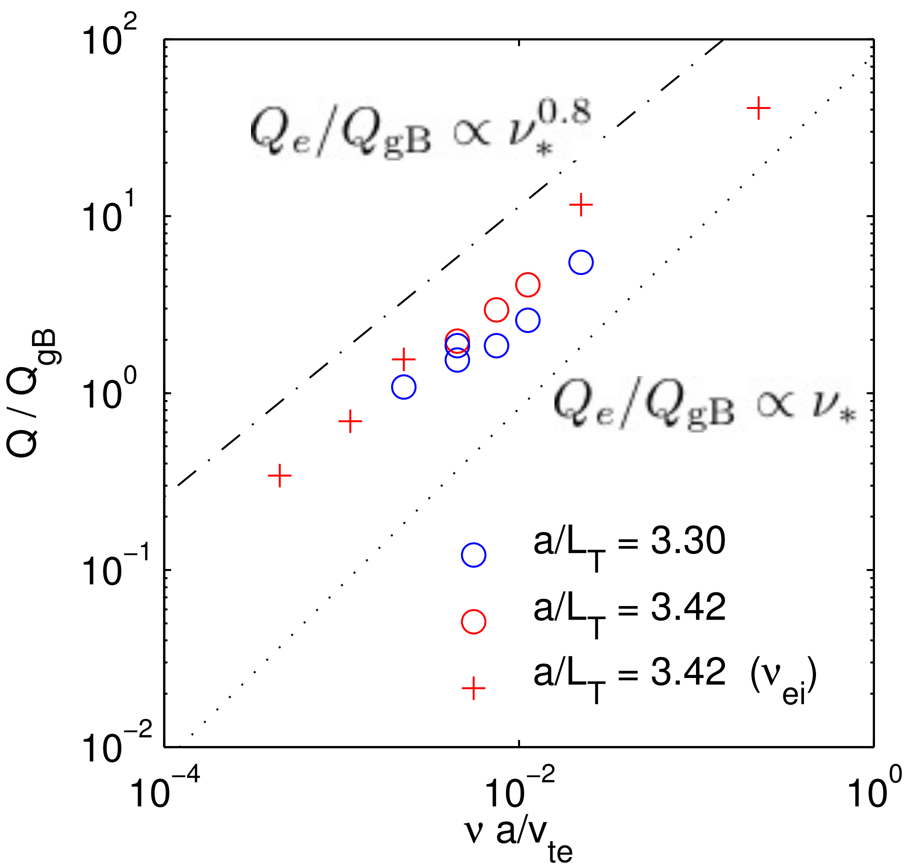

G. J. Colyer et al. 2017, PPCF 59, 055002

Conclusions

- Electrostatic GK with kinetic electrons adequately describes ion-scale turbulence in the presence of flow shear in MAST.
- This turbulence is subcritical.
- The transition to turbulence occurs via an intermediate state dominated by long-lived coherent structures, which become more numerous away from threshold until eventually overlapping, breaking up and turning into vanilla ITG turbulence.
- Experiment appears to sit at the boundary of these regimes.
- Tilted correlation functions and skewed density distributions are distinctive properties of the near-threshold regime. Symmetry is restored away from the threshold.

- ETG turbulence near threshold has a long-time saturated regime dominated by zonal flows, rather than settling in the usual "streamery" state.
- Heat flux in this regime scales linearly with collisionality, consistent with experimental scaling reported for MAST; the origin of this scaling is the slow decay rate of the zonal flows set by collisional viscosity.

F. van Wyk et al. 2016, JPP 82, 905820609
F. van Wyk et al. 2017, PPCF 59, 114003
M. F. J. Fox et al. 2017, PPCF 59, 034002
G. J. Colyer et al. 2017, PPCF 59, 055002

doi:10.1017/S0022377816001148

Transition to subcritical turbulence in a tokamak plasma

F. van Wyk[1,2,3,†], E. G. Highcock[1,4], A. A. Schekochihin[1,5], C. M. Roach[2], A. R. Field[2] and W. Dorland[1,6]

[1]Rudolf Peierls Centre for Theoretical Physics, University of Oxford, Oxford OX1 3NP, UK

[2]CCFE, Culham Science Centre, Abingdon OX14 3DB, UK

[3]STFC Daresbury Laboratory, Daresbury WA4 4AD, UK

[4]Chalmers University of Technology, Department of Physics, Göteborg SE-412 96, Sweden

[5]Merton College, Oxford OX1 4JD, UK

[6]Department of Physics, University of Maryland, College Park, MD 20742-4111, USA

(Received 23 September 2016; revised 23 November 2016; accepted 24 November 2016)

Tokamak turbulence, driven by the ion-temperature gradient and occurring in the presence of flow shear, is investigated by means of local, ion-scale, electrostatic gyrokinetic simulations (with both kinetic ions and electrons) of the conditions in the outer core of the Mega-Ampere Spherical Tokamak (MAST). A parameter scan in the local values of the ion-temperature gradient and flow shear is performed. It is demonstrated that the experimentally observed state is near the stability threshold and that this stability threshold is nonlinear: sheared turbulence is subcritical, i.e. the system is formally stable to small perturbations, but, given a large enough initial perturbation, it transitions to a turbulent state. A scenario for such a transition is proposed and supported by numerical results: close to threshold, the nonlinear saturated state and the associated anomalous heat transport are dominated by long-lived coherent structures, which drift across the domain, have finite amplitudes, but are not volume filling; as the system is taken away from the threshold into the more unstable regime, the number of these structures increases until they overlap and a more conventional chaotic state emerges. Whereas this appears to represent a new scenario for transition to turbulence in tokamak plasmas, it is reminiscent of the behaviour of other subcritically turbulent systems, e.g. pipe flows and Keplerian magnetorotational accretion flows.

Key words: fusion plasma, plasma instabilities, plasma simulation

Where to Publish a Plasma Physics Result That You Are Proud Of:

CAMBRIDGE UNIVERSITY PRESS

- ✓ No page limits or page charges
- ✓ Single-column format for beauty and e-reading
- ✓ **Organic locally sourced UK copy-editing/typesetting** (we won't ruin your algebra and we'll improve your grammar!)
- ✓ Direct 1-click access from NASA ADS; arXiv-ing encouraged
- ✓ Free access to highest-cited papers and featured articles
- ✓ **Interaction with a real editor of your choice, not a robot** (protection against random/stupid referees)

EDITORS: Bill Dorland (Maryland)
Alex Schekochihin (Oxford)

EDITORIAL BOARD:

Plasma Astrophysics: Jon Arons (Berkeley), Roger Blandford (Stanford), Dmitri Uzdensky (UC Boulder)
Space Plasmas: Francesco Califano (Pisa), Thierry Passot (OCA Nice)
Astrophysical Fluid Dynamics: Steve Tobias (Leeds)
Magnetic Fusion: Peter Catto (MIT), Per Helander (IPP Greifswald), Piero Martin (Padua), Paolo Ricci (Lausanne)
Dusty Plasmas: Ed Thomas Jr (Auburn)
HEDP: Antoine Bret (Castilla La Mancha), Mark Herrmann (NIF), Luis Silva (IST Lisbon)
Basic Lab Plasmas: Troy Carter (UCLA), Cary Forest (UW Madison)

When you submit a paper to JPP, you are putting your trust into the judgment of these editors, not anonymous reviewers, professional administrators or commercial imperatives

http://journals.cambridge.org/plasma

J. Plasma Phys. (2017), *vol.* 83, 715830403 © Cambridge University Press 2017
doi:10.1017/S0022377817000538

Three-dimensional magnetohydrodynamic equilibria with continuous magnetic fields

S. R. Hudson[1,†] and B. F. Kraus[1]

[1]Princeton Plasma Physics Laboratory, PO Box 451, Princeton NJ 08543, USA

(Received 21 April 2017; revised 27 June 2017; accepted 28 June 2017)

A brief critique is presented of some different classes of magnetohydrodynamic equilibrium solutions based on their continuity properties and whether the magnetic field is integrable or not. A generalized energy functional is introduced that is comprised of alternating ideal regions, with nested flux surfaces with an irrational rotational transform, and Taylor-relaxed regions, possibly with magnetic islands and chaos. The equilibrium states have globally continuous magnetic fields, and may be constructed for arbitrary three-dimensional plasma boundaries and appropriately prescribed pressure and rotational-transform profiles.

Key words: magnetized plasmas, plasma energy balance

J. Plasma Phys. (2017), *vol.* 83, 905830304 © Cambridge University Press 2017
doi:10.1017/S002237781700037X

Gyrokinetic continuum simulation of turbulence in a straight open-field-line plasma

E. L. Shi[1,†], G. W. Hammett[2], T. Stoltzfus-Dueck[1,3] and A. Hakim[2]

[1]Department of Astrophysical Sciences, Princeton University, Princeton, NJ 08544, USA

[2]Princeton Plasma Physics Laboratory, Princeton, NJ 08543-0451, USA

[3]Max-Planck-Princeton Center for Plasma Physics, Princeton University, Princeton, NJ 08544, USA

(Received 25 January 2017; revised 26 April 2017; accepted 27 April 2017)

Five-dimensional gyrokinetic continuum simulations of electrostatic plasma turbulence in a straight, open-field-line geometry have been performed using a full-f discontinuous-Galerkin approach implemented in the Gkeyll code. While various simplifications have been used for now, such as long-wavelength approximations in the gyrokinetic Poisson equation and the Hamiltonian, these simulations include the basic elements of a fusion-device scrape-off layer: localised sources to model plasma outflow from the core, cross-field turbulent transport, parallel flow along magnetic field lines, and parallel losses at the limiter or divertor with sheath-model boundary conditions. The set of sheath-model boundary conditions used in the model allows currents to flow through the walls. In addition to details of the numerical approach, results from numerical simulations of turbulence in the Large Plasma Device, a linear device featuring straight magnetic field lines, are presented.

Key words: plasma heat loss, plasma sheaths, plasma simulation

J. Plasma Phys. (2017), *vol.* 83, 905830504 © Cambridge University Press 2017
doi:10.1017/S0022377817000708

On non-local energy transfer via zonal flow in the Dimits shift

Denis A. St-Onge[1,2,†]

[1]Department of Astrophysical Sciences, Princeton University, Princeton, NJ 08544, USA

[2]Princeton Plasma Physics Laboratory, P.O. Box 451, Princeton, NJ 08543, USA

(Received 18 April 2017; revised 29 August 2017; accepted 30 August 2017)

The two-dimensional Terry–Horton equation is shown to exhibit the Dimits shift when suitably modified to capture both the nonlinear enhancement of zonal/drift-wave interactions and the existence of residual Rosenbluth–Hinton states. This phenomenon persists through numerous simplifications of the equation, including a quasilinear approximation as well as a four-mode truncation. It is shown that the use of an appropriate adiabatic electron response, for which the electrons are not affected by the flux-averaged potential, results in an $\boldsymbol{E}\times\boldsymbol{B}$ nonlinearity that can efficiently transfer energy non-locally to length scales of the order of the sound radius. The size of the shift for the nonlinear system is heuristically calculated and found to be in excellent agreement with numerical solutions. The existence of the Dimits shift for this system is then understood as an ability of the unstable primary modes to efficiently couple to stable modes at smaller scales, and the shift ends when these stable modes eventually destabilize as the density gradient is increased. This non-local mechanism of energy transfer is argued to be generically important even for more physically complete systems.

Key words: fusion plasma, plasma instabilities, plasma nonlinear phenomena